EXPERIMENTAL AND KINETIC ANALYSIS OF ACETALDEHYDE LOW-TEMPERATURE OXIDATION USING A RAPID COMPRESSION MACHINE

The present work was submitted to the Faculty of Mechanical Engineering

of the RWTH Aachen

Bachelor thesis

by

Alvaro Pamplona de Uña

Professor:	Prof. Dr.-Ing. Karl Alexander Heufer
Supervisor:	Prof. Dr.-Ing. Karl Alexander Heufer
Co-supervisor:	Jesús Caravaca Vilchez
Datum:	22. October 2024

Acknowledgement

First and foremost, I would like to express my sincere gratitude to Professor Heufer for giving me the opportunity to write my bachelor thesis at the HGD Institute in Aachen. I am very grateful for his support throughout this process. I would also like to extend my heartfelt thanks to my co-supervisor, Jesús Caravaca, whose guidance, support, and expertise were invaluable throughout the course of this project. His mentorship introduced me to the fundamentals of ignition delay and combustion processes, as well as the operating techniques of a rapid compression machine. Under his guidance, I not only gained a deeper understanding of the subject, but also experienced the day-to-day workings of research in this field. Finally, I would like to thank RWTH Aachen University for giving me the opportunity to study abroad and successfully complete my first engineering degree.

Contents

Figures

Tables

Schemes

Abbreviations

Jet stirred reactor	-	JSR
Shock tube	-	ST
Rapid compression machine	-	RCM
Ignition delay time	-	IDT
First stage	-	FS
Negative temperature coefficient	-	NTC
End of compression	-	EOC
End of compression pressure	-	Pc
End of compression temperature	-	Tc
Equivalence ratio	-	ϕ
Heat capacity	-	Cp
Hydrogen atom abstraction	-	HAA
Rate of production	-	ROP
Very low temperature	-	LLT
Low temperature	-	LT
Medium temperature	-	MT
High temperature	-	HT

Abstract

Acetaldehyde is a key intermediate in the combustion of biofuels. Previous research has investigated acetaldehyde combustion using several experimental methods, such as species concentration measurements in jet stirred reactors (JSR), ignition delay times (IDTs) in rapid compression machines (RCM) and shock tubes (ST), and flame velocities. However, there is a notable gap in the literature regarding measurements at low temperatures, particularly where IDT data are not available. To address this, we performed IDT measurements using an RCM at low temperatures, focusing on two end-of-compression pressures (10 and 20 bar) and two equivalence ratios (ϕ = 1.0 and 1.5). Comprehensive kinetic models from literature were evaluated against the measured data. The results showed significant discrepancies in the predictions, particularly in the lower temperature range (600-700 K). In contrast, at higher temperatures (above 900 K) the predictions were reasonably accurate for both the NUIGMech1.3 and Tao mechanisms, highlighting the need for further investigation into the low-temperature oxidation of acetaldehyde. To investigate this further, rate of production (ROP) analyses were carried out at the conditions studied using the best available mechanism: NUIGMech1.3. These analyses revealed that the primary pathway of acetaldehyde consumption at low temperatures is the abstraction of hydrogen atoms (HAA) at the alpha position, resulting in the formation of CH_3CO radicals, which are subsequently involved in addition to O_2. At higher temperatures the CH_3CO radicals decompose predominantly into CH_3 and CO, indicating a shift in the reaction mechanism with temperature. In addition, sensitivity analyses were performed to identify the reactions that most significantly influence the reactivity of acetaldehyde. This analysis revealed that CH_3CO_3 radical chemistry plays a crucial role in determining the reactivity of acetaldehyde. Species formed during the consumption of CH_3CO_3, such as methoxy radicals and peracetic acid, actively promote the reactivity of acetaldehyde. At higher temperatures, reactions following the HAA at the beta position of acetaldehyde, leading to the formation of CH_2CHO radicals, become increasingly relevant, with CH_2CHO radical decomposition playing a particularly important role. This information was used to modify NUIGMech1.3 model to enhance its performance in the low temperature regime. The rate coefficients for four key reactions, which were most sensitive in the low-temperature regime, were adjusted based on calculated and measured rates from the literature. ROP analysis showed that these rate adjustments resulted in increased production of CH_3CO_3 radicals, which significantly increased the reactivity of acetaldehyde at low temperatures. As a result, the modifications led to more accurate predictions of both acetaldehyde auto-ignition behavior and species formation in the low temperature range (below 750 K). This improvement highlights the importance of CH_3CO_3 radical chemistry in driving acetaldehyde oxidation under these conditions. However, in the medium temperature range, some important species were overpredicted. Despite these improvements, the study concludes that further research is necessary to develop a fully reliable model for acetaldehyde combustion, especially in the low-to-medium temperature regime. This study emphasizes the critical need for providing IDT validation targets using RCMs to refine kinetic models.

1 Introduction

1.1 Why Acetaldehyde?

Global warming has become a pressing issue that is causing widespread concern in society and is known that needs to be treated [1]. In response, biofuels are being developed to reduce greenhouse gas emissions and combat climate change. However, one challenge is the formation of acetaldehyde, a highly toxic and carcinogenic intermediate [2], during the combustion of biofuels in internal combustion engines. Acetaldehyde is also formed during the combustion of natural gas and alcohol-blended gasoline fuels. By studying the combustion chemistry of acetaldehyde, we aim to gain a deeper understanding of its formation and behavior, which can help optimize existing technologies and develop new strategies to minimize its emissions, ultimately contributing to cleaner and more sustainable energy solutions.

1.2 State of the art

Previous studies have investigated the combustion chemistry of acetaldehyde using experimental facilities such as jet stirred reactors (JSR), shock tubes (ST) and rapid compression machines (RCM). Both ST and RCM facilities have widely been used to investigate the auto-ignition behavior of several species, providing essential validation targets for model validation such as ignition delay times. Ignition delay time (IDT) is the time needed for a mixture of fuel and oxidizer to react at a certain temperature and pressure. This parameter provides valuable information to optimize engine operation.

ST have long been used to study both oxidation and pyrolysis of various species in the high temperature range [3]. Dagaut et al. [4] measured the IDT in a shock tube under a range of conditions: equivalence ratios $0.5 \leq \phi \leq 2$, temperatures between 1230-2530 K, and pressures of 2-5 atm. Similarly, Yasunaga et al. [5] conducted IDT experiments in the high temperature range (1250 K - 1800 K), focusing on both oxidation and pyrolysis of acetaldehyde. These studies revealed that sub-mechanisms involving methane, ethylene, ethane, formaldehyde, and ketene play a key role in the oxidation of acetaldehyde. Following similar work by Yasunaga et al. [5], Mèvel et al. [6] developed a model using new ST experiments and data from the literature, focusing on the high temperature regime. In addition, Hidaka et al. [7] studied acetaldehyde pyrolysis in a shock tube between 1000 and 1720 K at pressures between 1.2 and 3 bar and developed a 58-reaction mechanism capable of reproducing their measured data. Bentz et al. [8] extended this work by studying acetaldehyde decomposition in the range of 1250-1650 K at pressures between 1 and 5 bar, ultimately proposing a new equation to accurately describe the reaction kinetics of the acetaldehyde decomposition and the CH3CHO + H reaction. In addition, Won et al. [9] studied acetaldehyde shock waves in the temperature range of 1320 to 1897 K at 100 torr and concluded that at high temperatures the main oxidation pathways were the Rice-Herzfeld mechanism, the decomposition and oxidation of HCO and the reaction of H with O_2. Shrestha et al. [10] studied in a ST the oxidation kinetics of acetaldehyde and its interaction with NOx in the range of 1149 to 1542 K. In this study

was observed that the doping of NO over acetaldehyde did not modify the negative temperature coefficient (NTC) behavior.

RCM has been extensively used for a long time in previous oxidation studies at low temperatures [11]. Tao et al. [12] performed IDT experiments in a RCM between 700 K and 1100 K at 10 bar pressure. The results showed an NTC behavior, which is explained by the change of the reaction pathway of CH_3 radicals with temperature. Based on this data, and their previous JSR study [15], they developed a kinetic model for acetaldehyde oxidation capable of reproducing its NTC behavior to some extent. Recently Najafi et al. [13] studied the IDT methane with small portions of acetaldehyde at elevated pressure using a RCM, at 60 bar as combustion pressure between 750 and 900 K with fuel-air equivalence ratios between 1 and 4. The inclusion of small amounts of acetaldehyde was observed to significantly increase the reactivity of methane.

The IDT represents a macroscopic property of the mixture under study. For a comprehensive validation of kinetic models, more intrinsic validation targets, such as species concentration measurements, are desirable. As mentioned above, species measurements in shock tubes have already been reported, mainly under pyrolysis conditions. However, in the low temperature regime, other experimental setups such as flow reactors have been used to further investigate the oxidation of acetaldehyde. Dagaut et al. [4] studied the combustion of acetaldehyde in a JSR in the range of high temperature between 950 K and 1350 K and pressure range between 1-10 atm. After taking samples and analyzing them at a GC they obtained relevant intermediate species concentration profiles. Zhang et al. [14] measured the speciation in the oxidation in a JSR between 460 K and 900 K, equivalence ratios between 0.5 to 4.0 and pressures between 710 and 720 Torr. Using this data and the calculated H-atom abstraction rates, they designed an acetaldehyde mechanism that successfully met a wide range of available validation targets. Tao et al. [15] studied the NTC in the low-temperature (528-946 K) regime in the oxidation of acetaldehyde. These JSR studies concluded that the occurrence of addition to O_2 of CH_3CO and the decomposition of CH_3CO was the cause of this NTC behavior. Hashemi [16] developed a kinetic model in the range of intermediate to high temperature and high pressure. To achieve this goal, flow reactor experiments and IDT measurements in shock tube were carried out and JSR data in the available literature was used to compare predictions and experiments.

Species concentrations and laminar burning velocities have been measured experimentally in high-temperature flames. Fuels with higher laminar burning velocities are expected to exhibit accelerated combustion rates in engine applications, contributing to improved combustion efficiency [17]. Leplat et al. [18] studied three different stabilized flames using acetaldehyde as a fuel, at a pressure of 50 mbar and with equivalence ratios of 0.75, 1 and 1.25. In their study, several mechanisms were tested and they proposed improvements to Marinov's mechanism [19], where an ethanol kinetic model was developed. Christensen et al. [20] later measured the laminar burning velocities of acetaldehyde and compared their results with the predictions of several mechanisms in the literature. They concluded that Leplat's model [18] was the most

accurate and found that the discrepancies between experiment and prediction were not due to fuel-specific reactions. Subsequently, Tao et al. [21] investigated the chemical structure of a low-pressure laminar acetaldehyde flame with equivalence ratios of 1 and 1.7, in which molar fraction profiles of 40 species were reported and provided further insight into the development of future mechanisms.

1.3 Motivation and contents of this work

Despite extensive research on the oxidation of acetaldehyde, studies at low temperatures close to engine operation are scarce. While JSR studies provide valuable insight into the formation of intermediates at low temperatures, they are limited to low pressure and/or highly dilute environments. However, for the development of comprehensive and robust kinetic models, further measurements at engine-relevant conditions are desirable, highlighting the need to perform experiments using an RCM. In this work, we conducted IDT experiments in an RCM under conditions ranging from 10 to 20 bar, with ϕ values of 1 and 1.5. We evaluated the most comprehensive acetaldehyde kinetic models against the experimental data. The consumption pathways of acetaldehyde were analyzed using the best performing mechanism, followed by various sensitivity analyses to identify the most critical reactions in its consumption. Finally, based on the findings of the previous sections, comprehensive modifications were made to improve the performance of the selected mechanism. The proposed model was then validated against the measured data and existing IDT and JSR data from the literature.

2 Methodology – Rapid compression machine

In this work, IDT experiments were carried out in an RCM at two different pressures: 10 and 20 bar. The equivalence ratio was also varied with values of 1 and 1.5. The specific conditions under which the experiments were conducted are detailed in Table 1.

Table 1. Experimental mixture conditions.

Mix. Nº	Molar Composition (%)			Pc (bar)	ϕ
	CH_3CO	O_2	Diluents		
M1	2.778	6.944	90.278	10	1.0
M2	2.778	6.944	90.278	20	1.0
M3	4.11	6.849	89.041	20	1.5

The design and construction of the RCM used in this study has been described in detail by Lee et al. [22]. In brief, the machine uses a pneumatic drive mechanism coupled with a hydraulic stop and reactor segment, as seen in Figure 1 (top). The reactor serves as the actual test section where combustion and all relevant measurements are conducted. In the reactor, a Kistler pressure transducer is used to monitor pressure dynamics during IDT experiments. The ignition delay time is defined as the interval between the end of compression (EOC) and the maximum pressure rise associated with auto-ignition. Both first-stage onset and main ignition are identified at the largest pressure increase (max dP/dt) induced by the corresponding ignition event (first-stage or main ignition). In Figure 1 (bottom) a typical example of an IDT experiment is seen. IDTs were measured in a range from about 2 ms to about 160 ms.

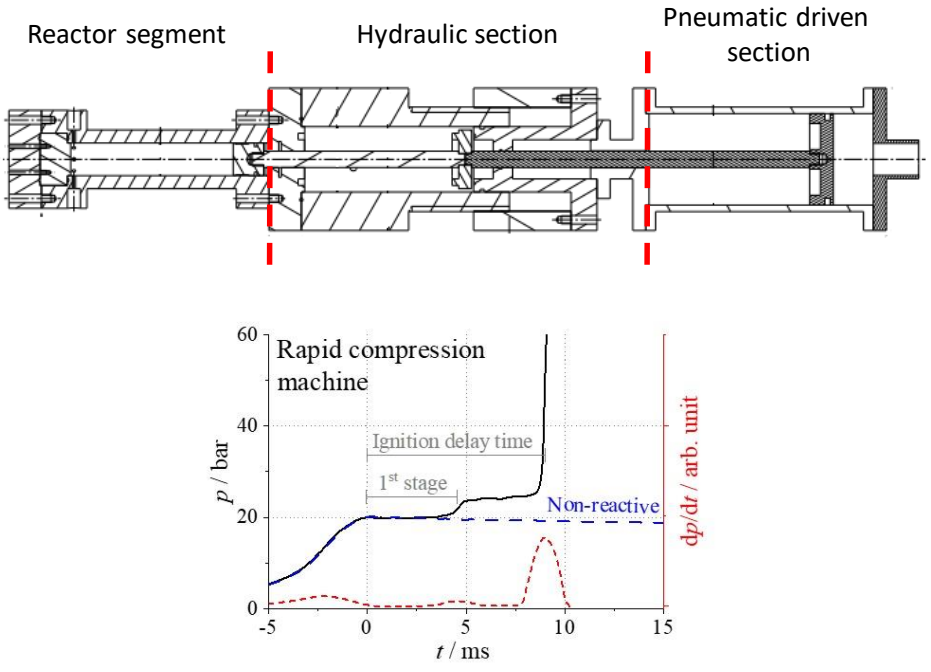

Figure 1. HGD RCM construction (top) and characteristic IDT experiment in the presence of first stage (bottom).

The EOC temperature is calculated using isentropic compression relations based on the adiabatic core hypothesis and the measured pressure (equation 1). A moving endwall was used to change the compression ratio, which in turn changes the end-of-compression temperature. Despite of that, four different bath gas compositions were required to cover the full temperature range. For the temperatures between 900 K and 1200 K (HT regime) a bath gas composition of 100% Ar was used. For temperatures between 900 K and 750 K (MT regime) a bath gas composition of 50% N_2 and 50% Ar was used. Between 750 K and 640 K (LT regime) the bath gas composition was 95% N_2 and 5% Ar. For the temperatures 640 K to 600 K (LLT regime) the composition was 30% CO_2 and 70% N_2. All these bath gas compositions are listed in Table 2. Mixture preparation was performed in stainless-steel mixing vessels, with the partial pressures of the individual gases monitored by two pressure sensors with ranges of 0-500 mbar and 0-10 bar (STS ATM.1). The mixtures were prepared in two separate vessels: one for the reactive mixture and the other for the non-reactive mixture. After both mixtures were prepared, a 20 minute period was allowed to ensure proper homogenization before proceeding with the experiments. The manifold and reactor were heated to 30ºC to ensure that the acetaldehyde remained in the gas phase throughout the process, while reducing the risk of polymerization [23]. Uncertainty estimates using the Ramalingam et al. [24] method are ±5 K for temperature and ±0.15 bar for pressure.

$$ln\left(\frac{p_c}{p_i}\right) = \int_{T_i}^{T_c} \frac{\gamma}{\gamma - 1}\frac{dT}{T} \tag{1}$$

Table 2. Bath gas composition for different range of temperatures.

Composition	Range of temperature (K)	Molar Fraction (%)		
		N_2	Ar	CO_2
C1	900-1200	-	100	-
C2	750-900	50	50	-
C3	640-750	95	5	-
C4	600-640	70	-	30

Three representative reactive traces of acetaldehyde combustion are shown in Figure 2. The red trace corresponds to the HT regime, with the composition of C1. In this temperature range, due to the increased reactivity, IDTs are shorter. After the end-of-compression pressure peak, the curve rises rapidly, clearly indicating the main ignition. The black trace shows the curve of an experiment carried out in the MT range, using C2. In this temperature regime we observe first-stage heat release during the compression stroke. As a result of this early heat release, the target end of compression pressure,

originally set at 10 bar, increases to pressures above 11 bar. This makes it difficult to accurately determine the exact time of compression termination and consequently the ignition delay times, as previously noted by Tao et al. [12]. Therefore, ignition delay times are not reported in this temperature range. After the first-stage formation, heat loss and heat release balance. Following this equilibrium, heat release accelerates rapidly, marking the start of the main ignition. The blue trace shows a typical profile for an experiment in the LLT regime with a first and main stage heat release, where C4 was used. The curve shows an initial peak at the end-of-compression pressure, followed by a pressure drop due to heat loss. There is then a sharp rise, indicating the first stage of heat release, followed by a second corresponding to the main ignition event. It is important to note that pressure increases due to ignition are more moderate under these conditions, as the bath gas used in these low temperature experiments has a higher heat capacity ($CpCO_2$ > CpAr).

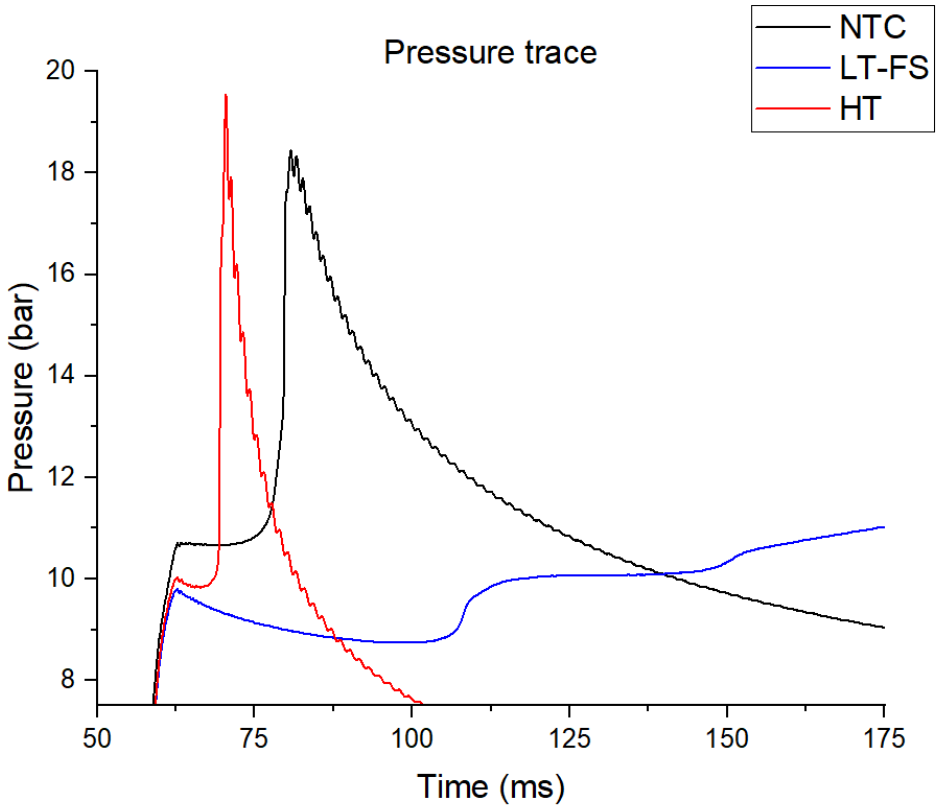

Figure 2. Pressure trace comparison of reactive experiments performed in a RCM with acetaldehyde as fuel. Blue trace represents a LLT experiment, black trace represents a MT experiment and red trace represents a HT experiment.

To accurately simulate the compression phase and heat loss in experiments, non-reactive mixture as introduced before is used under each condition. In these tests, oxygen (O_2) is replaced by nitrogen (N_2) and the resulting pressure profile is used to determine an effective volume profile. Using this information, zero-dimensional simulations of the IDTs were performed using custom scripts based on the Cantera software package [25].

3 Kinetic model comparison

Six comprehensive kinetic models have been tested in this work to determine the best mechanism available in the literature to predict the oxidation behavior of acetaldehyde. The simulations were carried out with input volumes of non-reactive experiments done at 10 bar and stochiometric conditions and allowed us to study two different parameters, IDT and FS. Figure 3 shows these results. The measured IDTs show a distinct S-shaped curve, characteristic of the NTC behavior observed in certain fuels, such as iso-octane or biofuels. In the mid temperature range, between 700 and 1000 K, the IDT increases with increasing temperature, reflecting the competition between low and high temperature chemical pathways[26]. Below 700 K and above 1000 K, acetaldehyde behaves more like an Arrhenius fuel, where the IDT decreases with increasing temperature. This is because only the low temperature chemistry dominates below 700 K and only the high temperature chemistry is active above 1000 K. It is important to note that the predictions with the 30% CO_2 - 70% N_2 mixture did not result in ignition for some of the existing mechanisms, and thus are not shown in the figure. The only mechanisms that shown ignition in at least two simulations within this range were NUIG1.1 [27-37] and Tao, and they are therefore represented.

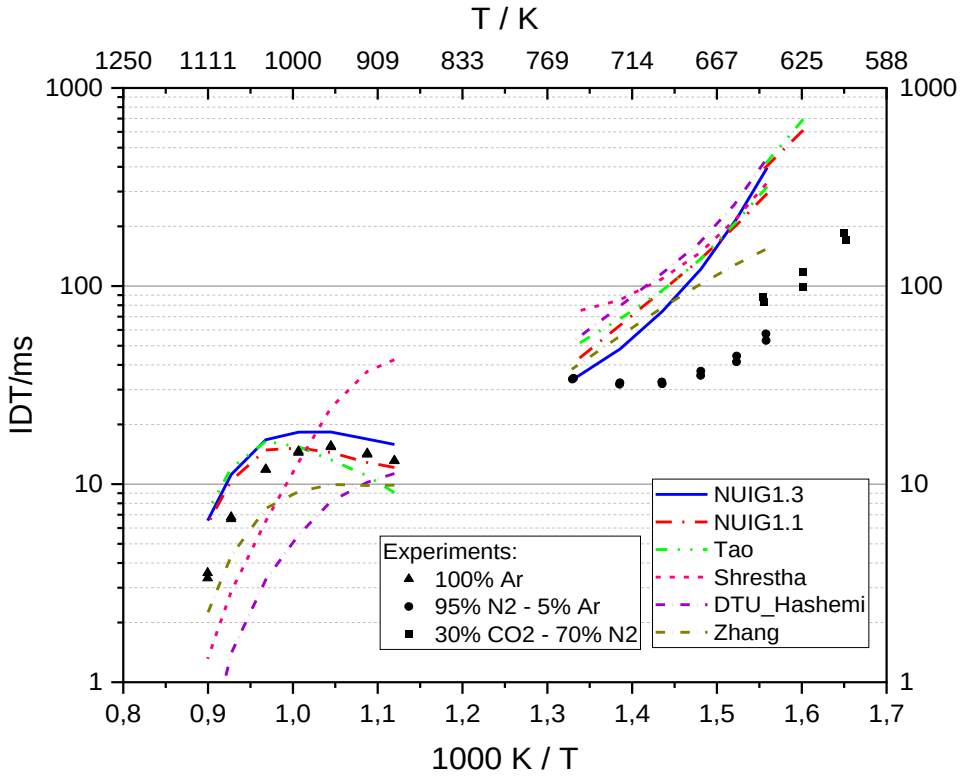

Figure 3. IDT experiments in a RCM and their simulation with different mechanisms in the available literature at Pc=10 bar.

The performance of the different mechanisms was evaluated over different temperature ranges. Tao and NUIG1.1 models showed similarities, particularly in the high temperature range (above 1000 K), where both predicted slightly longer IDTs. Between 900 K and

1000 K range, both models predicted the auto-ignition behavior of acetaldehyde in the NTC region reasonably well. NUIGMech1.3 [38-42] provides better IDT predictions between 700 and 770 K. However, at lower temperatures, all mechanisms predicted slower IDTs compared to the experimental data.

In contrast, the DTU-Hashemi mechanism lacks performance in both temperature regimes, underestimating IDT at high temperatures, resulting in faster than expected ignition, and overestimating the IDT at low temperatures, resulting in slower ignition. This mechanism also shows weaker NTC behavior than that showed by the experiments. A similar trend is observed in the Shrestha mechanism, where the Arrhenius behavior is even more pronounced at high temperatures. Zhang's mechanism is intermediate between the others, showing stronger NTC behavior than DTU and Shrestha, but weaker than Tao and NUIG. The high temperature discrepancies are mainly due to differences in the vinoxy radical chemistry. In the DTU and Shrestha models, the OH-forming pathway ($CH_2CHO + O_2 \rightarrow CH_2O + CO + OH$) dominates over the CH_3- and CO-forming decomposition pathways, whereas the opposite is true for the Tao and NUIG models. This shifts the balance towards increased OH formation, increasing the radical pool and therefore the reactivity of the mixture at high temperatures.

Overall, some of the available mechanisms perform reasonably well at high temperatures (> 900 K), in particular NUIGMech models and Tao's mechanism. However, at the lowest temperatures there are significant discrepancies for all models. As the temperature decreases, the predicted IDTs increase to a larger extent than the measured values, leading to significant deviations below 700 K. In some cases, such as the Shreshta model, the predicted reactivity is so low that no ignition is predicted. These large discrepancies between predictions and experimental data arise because most of these models were developed primarily using high temperature ignition delay times to describe the autoignition behavior of acetaldehyde. At lower temperatures, the only experimental data available are JSR measurements, as detailed in the introduction, resulting in poor predictions of its autoignition behavior in this temperature range.

Due to the significant heat release induced by the first-stage ignition, the adiabatic core assumption in the RCM may no longer hold after the first stage during IDT experiment. This potential breakdown of the adiabatic core hypothesis is currently the subject of ongoing discussion within the combustion research community. Prior to the first stage, the adiabatic core hypothesis is known to be fulfilled[43]. Therefore, more emphasis should be placed on the first stage ignition itself as a key validation target, rather than relying solely on the IDT. Figure 4 shows the comparison between measured and predicted first–stage ignition location at 10 bar and stoichiometric conditions. The performance of the DTU Hashemi, Shrestha, Tao and NUIG1.1 mechanisms are all comparable, with similar slopes and predictions that are approximately one order of magnitude slower than the experimental data. Zhang's mechanism predicts the fastest first stage ignition at lower temperatures; however, its performance is compromised upon closer examination of the slope, which deviates from the trend shown experimentally.

NUIGMech1.3, although also showing significant discrepancies in the predicted magnitude of FS onset, has a slope that is more consistent with the experimental data. Overall, none of the models accurately predict FS onset, and the discrepancies are even greater than those observed for IDT predictions. This highlights the lack of understanding of the low temperature chemistry of acetaldehyde. In the following section, this conclusion is evaluated using NUIGMec1.3 at different conditions of pressure and equivalence ratio.

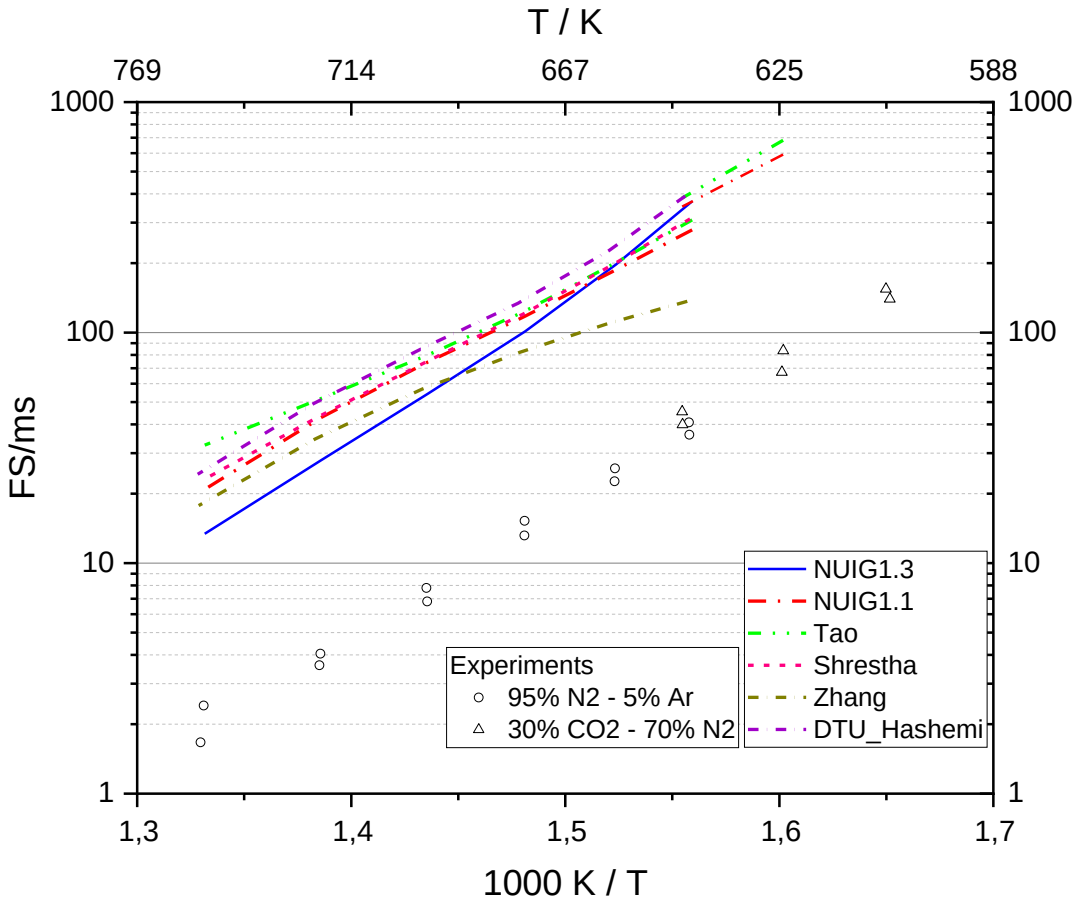

Figure 4. Experimental first stages and simulated first stage with different available mechanisms for Pc=10 bar.

3.1 Pressure and equivalence ratio influence

In this Section, we have investigated the influence of pressure and equivalence ratio (ϕ) on the oxidation behavior of acetaldehyde at low temperatures by comparing the experimental data measured in this work at the conditions listed in Table 1. The measured data is complemented with model predictions using the mechanism identified as the most accurate, NUIG1.3. These results are shown in Figure 5.

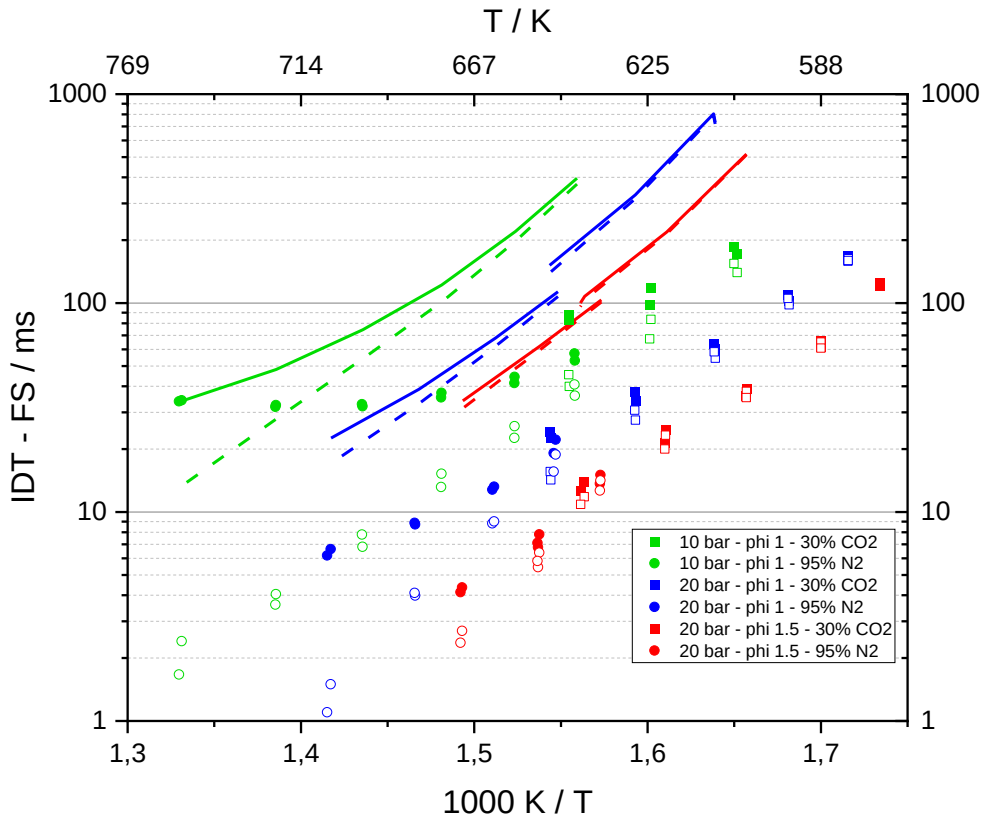

Figure 5. Experimental and simulated IDT and FS in a RCM**.** Symbols are the experiments carried out in a RCM. Filled symbols are IDT measures and empty symbols are FS measures. Lines are simulations. Continuous lines are simulated IDTs, and dashed lines are simulated FS.

The IDTs measured at 10 bar are significantly longer - over 100% longer - than those observed at 20 bar ($\phi = 1$). The data show a clear trend of decreasing IDTs with increasing pressure, consistent with behavior observed in other hydrocarbons [44]. Higher pressure allows for increased molecular interaction, which increases the concentration of reactants and, in turn, accelerates the rate of chemical reactions. In addition, higher pressure increases the production of key radicals that drive chain-branching reactions, leading to faster combustion. Similarly, the ignition delay times for experiments with $\phi = 1.0$ were longer than those with $\phi = 1.5$. Fuel rich mixtures ($\phi > 1$) have more fuel available, which can promote faster radical formation and chain branching reactions, leading to shorter ignition delay times. In addition, richer mixtures tend to increase heat release during combustion, further accelerating the ignition process.

Model predictions show discrepancies in both IDT and FS data at the investigated pressures and equivalence ratios, with a consistent trend towards underprediction of reactivity at low and very low temperatures (LT and LLT), as anticipated in the previous section. However, despite these discrepancies, the influence of pressure and equivalence ratio is well captured in the simulations. This further highlights the need for detailed kinetic modelling analysis on acetaldehyde specific chemistry.

4 Rate of production analysis

This section describes the oxidation network of acetaldehyde at moderate to high pressures, with a detailed discussion of the reaction fluxes. Scheme 1 illustrates the consumption pathways of acetaldehyde and the primary reaction fluxes within the network. In the oxidation of acetaldehyde, the initial steps are predominantly hydrogen atom abstraction (HAA) reactions. These reactions occur primarily at the α-position and, to a lesser extent, at the β-position of the acetaldehyde molecule. HAA at the α-position leads to the formation of the acetyl radical (CH_3CO), whereas abstraction at the β-position leads to the formation of the vinoxy radical (CH_2CHO). The formation of the acetyl radical is mainly driven by reactions with the methoxy radical (CH_3O) and the hydroxyl radical (-OH). In contrast, HAA in the β-position is mainly promoted by the hydroxyl radical (-OH).

CH_3CO radical then follows two pathways, an addition to O_2, in which is produced acetylperoxyl radical (CH_3CO_3) and at low temperatures it is consumed around 75% of the acetyl radical, and a radical decomposition ($CH_3 + CO$). The CH_3CO_3 radical then is consumed in four different pathways. First, CH_3CO_3 reacts with CH_3O_2 in a lumped step ($CH_3CO_3 + CH_3O_2 \rightarrow CH_3CO_2 + CH_3O + O_2$), forming the CH_3O radical, a crucial intermediate for the α-position HAA of acetaldehyde. This reaction constitutes the primary consumption pathway for CH_3CO_3. Second, CH_3CO_3 radicals undergo radical recombination to produce CH_3CO_2 radicals ($2\ CH_3CO_3 \rightarrow 2\ CH_3CO_2 + O_2$). The resulting CH_3CO_2 radical from these two pathways finally undergo decomposition into CH_3 and CO_2. The third most relevant pathway in the consumption of CH_3CO_3 is another radical-radical recombination reaction between CH_3CO_3 and CH_3O_2 ($CH_3CO_3 + CH_3O_2 \rightarrow CH_2O + CH_3COOH + O_2$). Finally, CH_3CO_3 is consumed by HAA at the β-position of acetaldehyde. This highlights the important role of CH_3CO_3 radicals, not only in reactions involving smaller radicals such as CH_3O_2, but also in driving key steps in acetaldehyde consumption.

A less important consumption pathway is the production of vinoxy radical from β-position HAA of acetaldehyde. The production of this intermediate only consumes around 5% of acetaldehyde (much fewer than the HAA at α-position). This radical is mostly consumed by an addition to O_2 at low temperatures, producing the O_2CH_2CHO radical. This radical then undergoes a five-membered ring isomerization to form HO_2CH_2CO which then suffers a total radical decomposition in $CH_2O + CO + OH$.

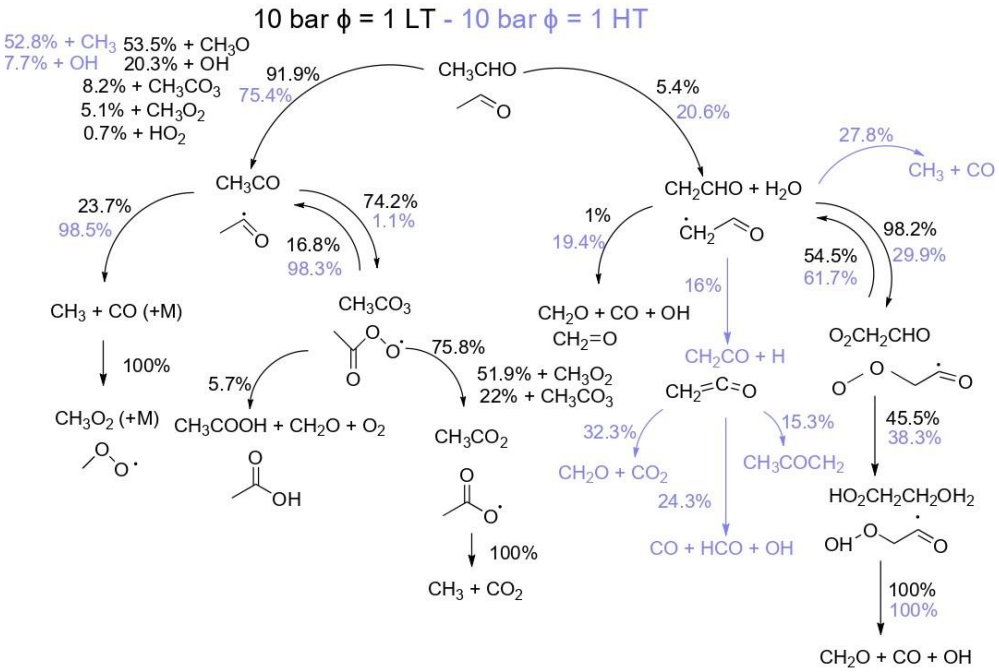

Scheme 1. Rate of production analysis, using NUIG1.3 mechanism when 10% of fuel is consumed under the following conditions: black color Pc = 10 bar, ϕ = 1 and Tc = 641 K and light blue for Pc = 10 bar, ϕ = 1 and Tc = 1089 K.

To assess the effect of temperature on acetaldehyde oxidation, we analyzed the reaction pathway at 1089 K. In light blue were also added in Scheme 1 new reaction pathways that did not exist at 641 K. At 1089 K, HAA from acetaldehyde at the β-position increases significantly, raising the conversion rate from 5% to 20%. Consequently, the HAA at the α-position decreases from a conversion rate of 90% to 75%. Despite this shift, the α-position HAA remains the dominant pathway for acetaldehyde consumption. A notable difference between high and low-temperature oxidation is the nature of the radicals involved in the α-position HAA. At higher temperatures, the most prominent α-position abstraction is driven by the methyl radical (CH_3), accounting for 52.8% of the reaction. In contrast, at lower temperatures, the methoxy radical (CH_3O) is primarily responsible for the α-position HAA of acetaldehyde (53.5%), as mentioned before. In addition, the radical decomposition of acetyl radical becomes much more prominent at high temperatures, increasing from around 24% at low temperatures to around 98% at high temperatures. This suggests that at elevated temperatures the decomposition pathway of the acetyl radical to CH_3 and CO predominates over the addition to O_2 mechanism.

A similar trend is observed with the products of HAA at the β-position. In the low-temperature range, the vinoxy radical (CH_2CHO) predominantly undergoes addition to O_2, with a conversion rate of 98.2%. However, at high temperatures, this reaction pathway drops to 30%. At high temperatures, three additional pathways for vinoxy radical consumption emerge. Radical decomposition to CH_3 and CO emerges as the dominant consumption pathway for the vinoxy radical, similar to that observed for the acetyl

radical. In addition, a ketene formation reaction ($CH_2CHO \rightleftharpoons CH_2CO + H$) and an OH formation pathway ($CH_2CHO + O_2 \rightarrow CH_2O + CO + OH$) become increasingly important in this temperature range. These observations suggest that while RO_2 chemistry is more relevant at lower temperatures, the importance of radical decomposition pathways increases with increasing temperature, as previously observed for other hydrocarbons.

In order to analyze the influence of pressure and equivalence ratio in the consumption pathway we studied the reaction pathways of two conditions: Pc=20 bar, ϕ=1 and Tc=641 K to assess the influence of the pressure and Tc and Pc=20 bar, ϕ=1.5 and Tc=641 K to assess the influence of the equivalence ratio (see Scheme 2). It was found that conversion ratios were very similar between them and no new relevant reaction was observed. It was therefore concluded that the branching ratios within the acetaldehyde oxidation network are not significantly affected by moderate variations in pressure and equivalence ratio.

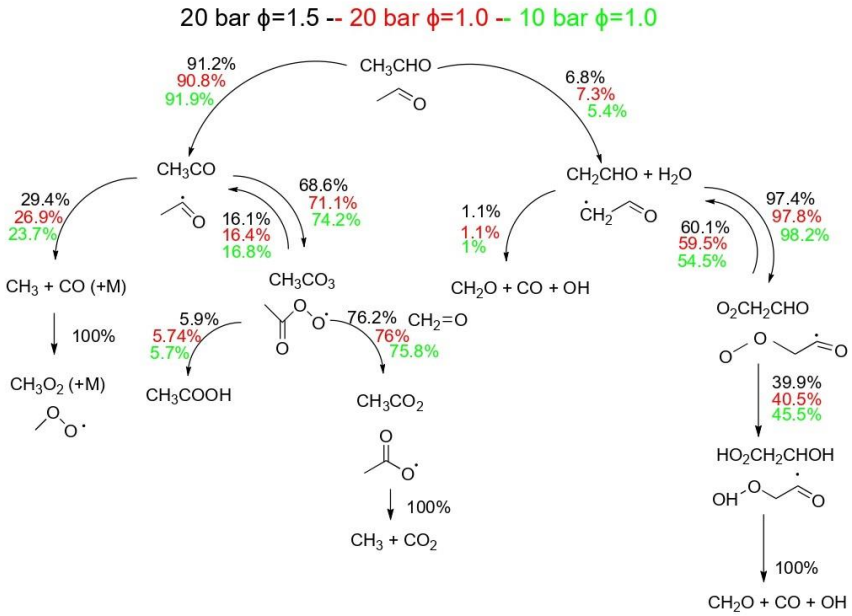

Scheme 2. ROP analysis comparing the influence of pressure and equivalence ratio at 641 K.

In the previous section, a comparative analysis of different kinetic mechanisms was carried out to evaluate their performance. Significant discrepancies were observed in the high to medium temperature range, where NUIGMech1.3 exhibited an NTC behavior, more in line with the experimental data. In contrast, the NTC behavior of the DTU mechanism was much weaker. However, in the low temperature range, no significant differences were found between the mechanisms. Consequently, a ROP analysis was performed (see Scheme 3) using mixture M1 at a temperature of 1078 K to assess the differences in high temperature chemistry between the two mechanisms (see Figure 3).

No significant differences were observed in the overall HAA conversion rates of acetaldehyde between the mechanisms studied, with differences remaining below 5%. Both mechanisms predict the complete decomposition of the CH_3CO radical into CH_3 and

CO. However, significant differences were observed in the chemistry of the CH_2CHO radical. In this case, the DTU-Hashemi mechanism predicts a conversion rate for $CH_2CHO + O_2 \rightarrow CH_2O + CO + OH$ almost three times higher than that of NUIGMech1.3 (70.4% in DTU-Hashemi vs. 24% in NUIGMech1.3). In contrast, NUIGMech1.3 favors the decomposition of the CH_2CHO radical into $CH_3 + CO$ and the formation of ketene ($CH_2CHO \rightleftharpoons CH_2CO + H$).

The $CH_2CHO + O_2 \rightarrow CH_2O + CO + OH$ pathway is particularly important because it produces OH radicals, which are essential for accelerating the oxidation process and thereby reducing the IDT. This explains why the DTU-Hashemi mechanism predicts significantly shorter IDTs and shows a trend that differs significantly from the experimental results, as shown in Figure 3.

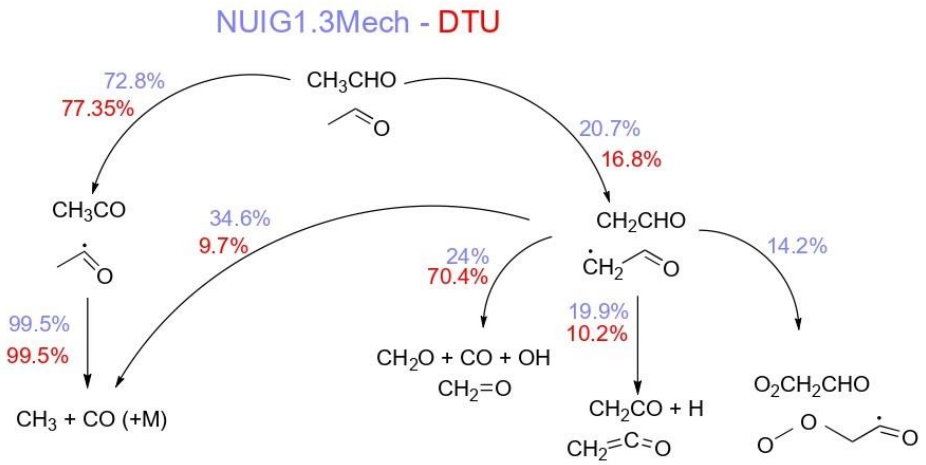

Scheme 3. ROP analysis at 10 bar and 1078 K, ϕ=1.0. Comparison of mechanisms at high temperature: NUIG1.3Mech in light blue and DTU Hashemi in red.

5 Sensitivity analysis

A sensitivity analysis was performed to identify the most influential reactions in the oxidation of acetaldehyde and to compare the differences under different conditions. The rate constant for each reaction is described by an Arrhenius equation: $k = A\,T^n\,exp(-Ea/RT)$, the unit for T is K. The definition of the sensitivity coefficient is taken from previous studies [45]. To calculate it, the pre-exponential factor (A) of a reaction is varied by multiplying it by two and dividing it by two. This results in two modified ignition delay times: IDT(*2) for the increased A factor and IDT(/2) for the decreased A factor. This results in three different ignition delay times for each reaction: IDT(base), which is the original value, IDT(*2), and IDT(/2). Finally, the sensitivity coefficient is obtained: $SC = \frac{IDT(*2)-IDT(/2)}{IDT(base)}$ In this context, a negative sensitivity coefficient indicates that increasing the rate of the reaction results in a shorter IDT, indicating that the reaction is accelerating the combustion process. Conversely, a positive sensitivity coefficient means that increasing the rate of the reaction results in a longer IDT, indicating that the reaction is slowing the combustion process.

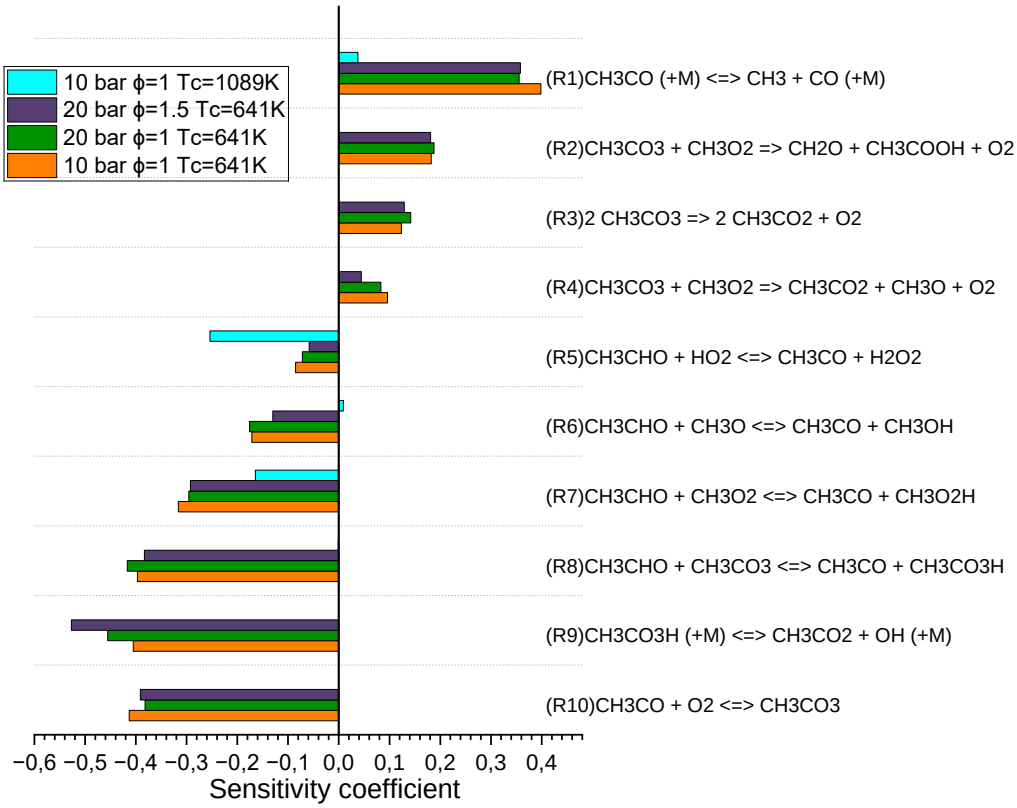

Figure 6. Sensitivity analysis on IDT with NUIG1.3mech mechanism at four conditions: 10 bar, ϕ=1 and Tc=641K; 10 bar, ϕ=1 and Tc=1089K; 20 bar, ϕ=1 and Tc=641K; 20 bar, ϕ=1.5 and Tc=641K. Reactions on the right are the most sensitive at 10 bar, ϕ=1 and Tc=641K.

Figure 6 shows the sensitivity analysis under four different conditions. The reference condition is set to Pc=10 bar, ϕ=1, and Tc=641K. The ten reactions shown in the figure are the most sensitive to this specific reference condition. The other bars show how

sensitive these top ten reactions are under the other conditions: ϕ=1 and Tc=1089K; Pc=20 bar, ϕ=1 and Tc=641K; Pc=20 bar, ϕ=1.5 and Tc=641K. The reader is referred to the numbering in Figure 6 for better interpretation of the following discussion. In R8, an HAA reaction results in the formation of CH_3CO_3H during the oxidation process. Subsequently, 96% of the CH_3CO_3H undergoes O-H bond cleavage in reaction R10, producing hydroxyl radicals (-OH). This pathway produces more OH radicals than it consumes, classifying these reactions as chain-branching. As a result, increasing the reaction rate of R8 and R10 would lead to an acceleration of the ignition process, as indicated by the negative sensitivity coefficient shown in Figure 6.

In reactions R5, R6, R7 and R8, HAA reactions lead to the formation of the CH_3CO radical. This radical is mainly consumed via two pathways: radical decomposition (R1) and addition to O_2 (R9). After addition to O_2, the resulting CH_3CO_3 radical can undergo three different transformations: radical decomposition (R4), radical recombination (R3), and decomposition back to CH_3CO and O_2. Reaction R3, $CH_3CO_3 + CH_3O_2 \rightarrow CH_3CO_2 + CH_3O + O_2$, leads to the production of CH_3O radicals. These CH_3O radicals are critical intermediates in acetaldehyde oxidation, with approximately 46% of acetaldehyde being consumed via HAA reactions involving these radicals. Specifically, in R6 ($CH_3CHO + CH_3O \rightleftharpoons CH_3CO + CH_3OH$), the formation of methoxy (CH_3O) radicals promotes acetaldehyde consumption. Therefore, the pathway $CH_3CHO + R \rightarrow CH_3CO_3 + CH_3O_2 \rightarrow CH_3CO_2 + CH_3O + O_2$ can be considered as chain branching pathway. Finally, CH_3CO_2 decomposes to CH_3 and CO_2. The chain branching pathway competes directly with the decomposition of CH_3CO_3 (R4), which leads to the formation of CH_3 and CO, similar to the previous pathway, but without the formation of methoxy radicals. This lack of methoxy radical formation explains why this pathway is considered to be one of the most important in inhibiting reactivity.

When comparing the sensitivity of the reactions shown in Figure 6, the most significant differences were observed with variations in temperature. Reactions that exhibited high sensitivity at 641 K lost their importance at 1089 K, except for the HAA reaction with HO_2 (R5), whose sensitivity coefficient increased at the higher temperature. This behavior is expected, as HO_2 chemistry becomes more prominent in the medium-to-high temperature regime. Only minor differences were observed between stoichiometric and rich conditions, with reactions such as the OH bond cleavage in peracetic acid (R9) becoming slightly more sensitive under rich conditions. When comparing different pressure levels, the most sensitive pathways at 10 bar showed similar sensitivity coefficients at 20 bar. However, the third-body reaction R9 reaction became more significant than the acetyl radical addition to O_2 (R10) at higher pressures. This can be explained by the fact that at higher pressures, the increased concentration of molecules increases the likelihood of these third-body collisions, thereby accelerating the reaction rate. The same degree of sensitivity across the different conditions is consistent with the similar conversion rates observed in the ROP analysis in the previous section.

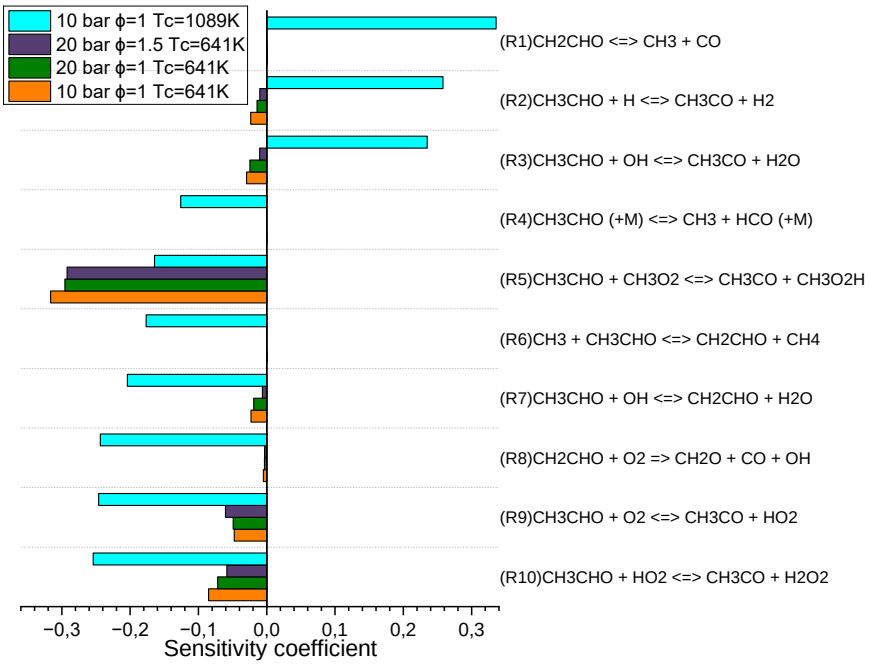

Figure 7. Sensitivity analysis on IDT with NUIG1.3mech mechanism at four conditions: 10 bar, ϕ=1 and Tc=641K; 10 bar, ϕ=1 and Tc=1089K; 20 bar, ϕ=1 and Tc=641K; 20 bar, ϕ=1.5 and Tc=641K. Reactions on the right are the most sensitive at 10 bar, ϕ=1 and Tc=1089K.

In Figure 7, the reactions with the highest sensitivity coefficients at elevated temperatures (10 bar, ϕ=1 and Tc=1089K) are shown and compared at the other conditions: 10 bar, ϕ=1 and Tc=641K; 20 bar, ϕ=1 and Tc=641K; 20 bar, ϕ=1.5 and Tc=641K. Reactions are numbered again from 1 to 10 for better understanding. Most of the reactions with high sensitivity coefficients at elevated temperatures show much lower sensitivity at low temperatures. The only reaction present in the top 10 at both high and low temperatures is the HAA by CH_3O_2 (R5), leading to the formation of CH_3CO radicals. This is due to the consistent production of CH_3 over the entire temperature range as shown in the ROP analysis from the previous section. The CH_3O_2 radical is predominantly formed by the third body reaction involving the addition of CH_3 to O_2.

The chemistry of CH_2CHO radicals become increasingly important at higher temperatures compared to lower temperatures. Reactions R6 and R7 exemplify HAA at the β-position leading to the formation of CH_2CHO radicals. These radicals are subsequently consumed in reactions R1 and R8, both of which involve radical decomposition processes. However, there are notable differences between the two pathways. In reaction R8, -OH radicals are generated which, due to their high reactivity, have a significant effect on the IDT. As a result, the R6-R8 pathway is classified as a chain-branching mechanism. This pathway competes with reaction R1, which produces a methyl radical and CO, both of which are less reactive than -OH radicals. This distinction explains the observation that R1 acts as the most inhibiting reaction at elevated temperatures.

It is noteworthy to observe the differences between reactions R2 and R3 compared to R9 and R10, all of which involve HAA at the α-position of acetaldehyde. While R2 and R3 inhibit the reactivity, R9 and R10 enhance it. This difference can be attributed to the fact that R9 and R10 lead to the formation of HO_2 and H_2O_2, which ultimately decompose to form highly reactive -OH radicals at these temperatures. In contrast, the competing reactions R2 and R3 primarily produce H_2 and HO_2, species with much lower reactivity. In addition, reaction R3, which involves HAA by –OH radicals, is not relevant at low temperatures. This is due to the dominance of HAA by methoxy radicals at low temperatures, as discussed above. Finally, reaction R4 represents direct decomposition of acetaldehyde, which is only relevant at high temperatures, as observed for other hydrocarbons [46].

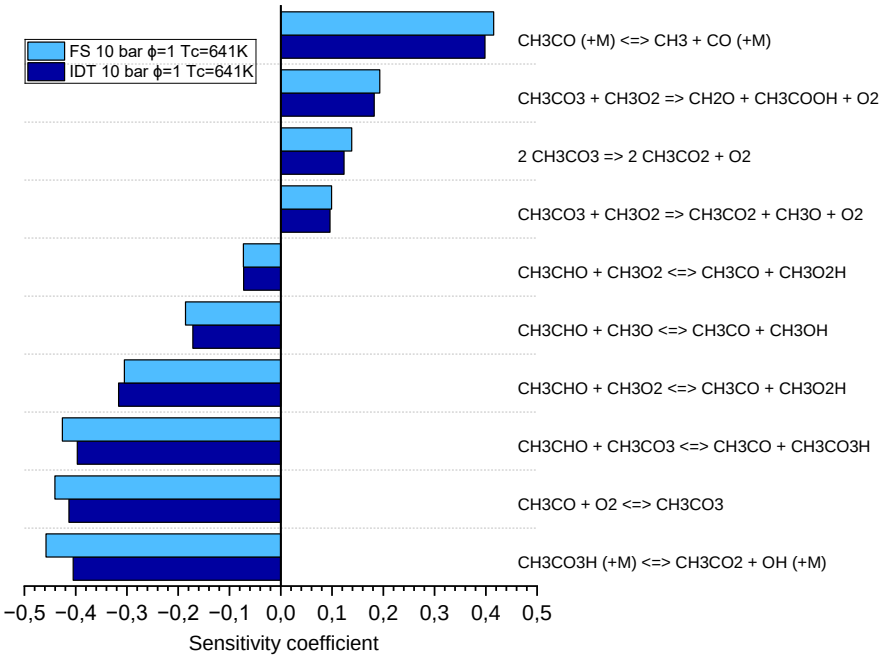

Figure 8. Sensitivity analysis on IDT and FS with NUIG1.3mech mechanism at 10 bar, ϕ=1 and Tc=641K.

For 10 bar, ϕ=1 and Tc=641K it was compared the sensitivity coefficient value of IDT against the FS. It is seen that not big differences are appreciated and in most cases the FS value is higher. Nevertheless, in the HAA at alpha-position of acetaldehyde (R6) it is seen how the sensitivity coefficient of the IDT is slightly higher than the FS coefficient. Based on the information gathered in this section and the ROP analysis, we propose modifications to the reaction rate constants to improve the performance of NUIGMech1.3, as seen in Figure 5. However, it is clear from the figure that the difference between the IDT and FS in the experimental data is significantly greater than the model predicts. This suggests that accurate prediction of both IDT and FS simultaneously would be challenging without adjustments to the thermochemistry.

6 Kinetic modelling suggestions

Based on the conclusions drawn from the ROP analysis (see section 4) and the sensitivity analysis, comprehensive modifications were made to the NUIG1.3 mechanism to improve its accuracy in modelling acetaldehyde oxidation. The purpose of this section is not to present a final, fully accurate kinetic model, but rather to provide insights and recommendations for improving the performance of existing kinetic models under low temperature conditions. The focus of this modelling analysis is limited to low temperature conditions as this is the range where the existing models showed the greatest discrepancies with experimental data, for both IDT and FS measurements. In particular, only rates for those reactions identified in the sensitivity analysis under the specific conditions shown in Figure 5 (Pc = 10 bar and ϕ = 1, low temperature) were considered in this analysis. The specific modifications made to the rate coefficients are detailed in Table 3. These modifications are illustrated in Figure 9, where the proposed changes are shown as solid lines. These rate constants, along with those utilized in the kinetic models analyzed in this work, are depicted as dashed lines in Figure 8.

The first modification involved the acetyl radical (CH_3CO) addition to O_2 (R10 in Figure 6). We replaced the rate coefficients of the NUIG1.3 mechanism with that of Tao's model. The rate was then increased by a factor of five (see Figure 8), leading to a significant increase compared to the original rate. In addition, the radical decomposition of CH_3CO (R1 in Figure 6) rate was decreased. We replaced the Arrhenius parameters of the NUIG1.3 model with those of the DTU Hashemi model and then halved the A factor. Finally, we increased the rates for both HAA of acetaldehyde at the α-position, specifically those involving CH_3O (R6) and CH_3CO_3 (R8) radicals. In the first case (R6) the DTU rate was used and then doubled, while in the second case (R8) the rate of the base mechanism was directly doubled. These modifications were made consistently within the reported uncertainty ranges of the corresponding reaction rates. The adjustments were specifically aimed at enhancing the reactivity predicted by the kinetic model at low temperatures. The performance of the revised mechanism was then evaluated under the conditions investigated in this study (see section 6.1 and section 6.2) and validated against literature targets (see section 6.3).

Table 3. Rate coefficients for modified reactions in this work.

Reaction	A (in cm, s and cal)	n	Ea (cal/mol)
$CH_3CO + O_2 <=> CH_3CO3$	2.54E+53	-12.96	1.156e+04
$CH_3CO <=> CH_3 + CO$	6.50E+19	-2.32	1.8012e+04
$CH_3CHO+ CH_3O<=> CH_3CO+ CH_3OH$	5.09E+04	2.578	249.4
$CH_3CHO + CH_3CO3 <=> CH_3CO + CH_3CO3H$	3.8316	3.6426	5641.9

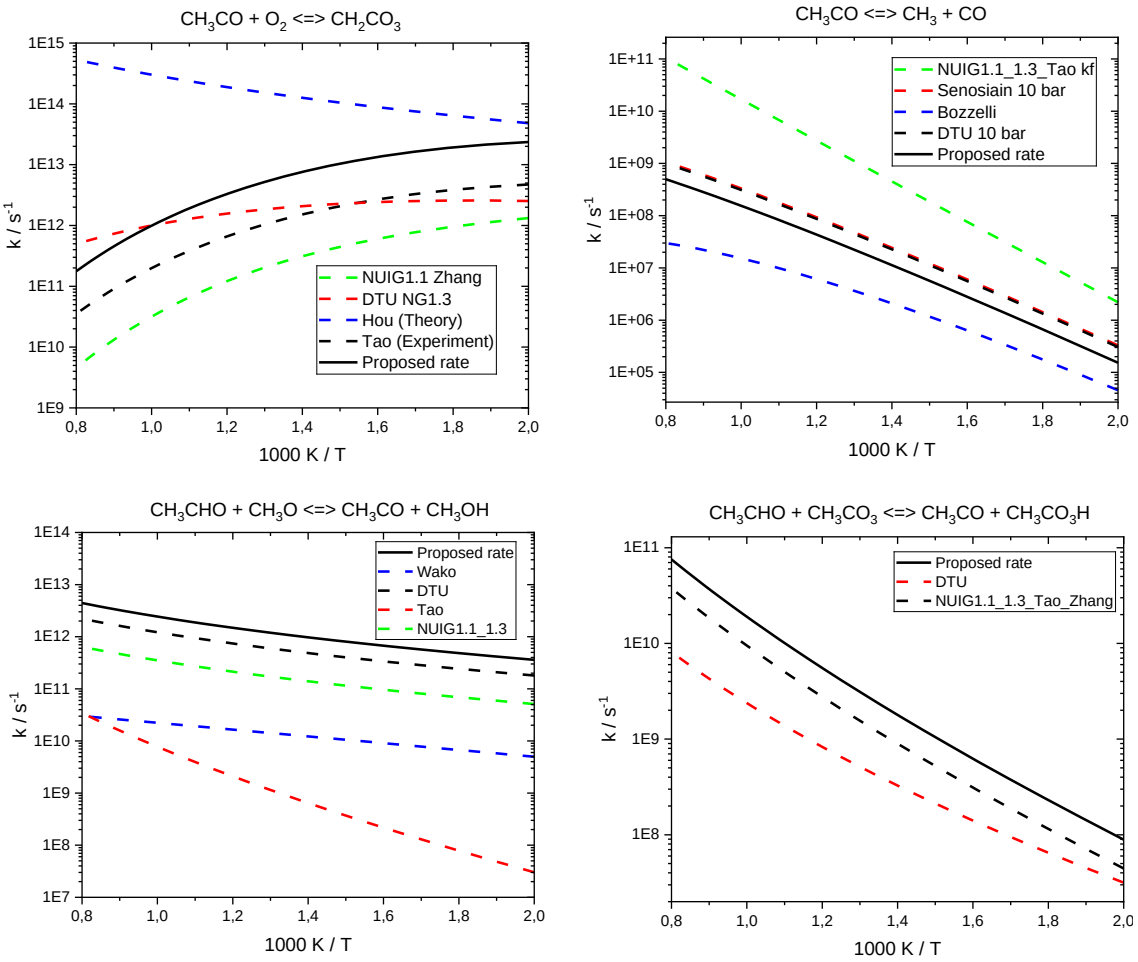

Figure 9. Comparison of the modified reaction rates with literature rates.

6.1 ROP analysis of proposed model

In this section, a ROP analysis was carried out to assess the impact of the changes outlined in Table 3 on the branching ratios within the acetaldehyde oxidation network. Scheme 4 presents a ROP analysis for the same experimental conditions as evaluated in Scheme 1, now comparing the results obtained from the original model with those obtained from the modified mechanism.

The first two modifications, that is increasing the rate of addition of the acetyl radical (CH_3CO) to O_2 (R10) and reducing the radical decomposition rate of the same species, CH_3CO, shifted significantly the branching ratios of the CH_3CO radical. The consumption pathway leading to CH_3CO3 increased from 74.2% to 95.3%, whereas the decomposition leading to CH_3 + CO decreased from 23.7% to 4.1%. This explains most of the observed increase in reactivity, since the first consumption pathway involves chain branching, as described in section 5. The other two modifications were the HAAs at the alpha position of acetaldehyde by methoxy (CH_3O) and CH_3CO_3 radicals. These adjustments resulted in a 14% increase in acetaldehyde consumption via HAA by CH_3O and an approximately 2% increase via HAA by CH_3CO_3. Both radicals are primary products of the acetyl radical

(CH_3CO) addition to O_2 pathway, highlighting the critical role of CH_3CO_3 chemistry in acetaldehyde oxidation at low temperatures.

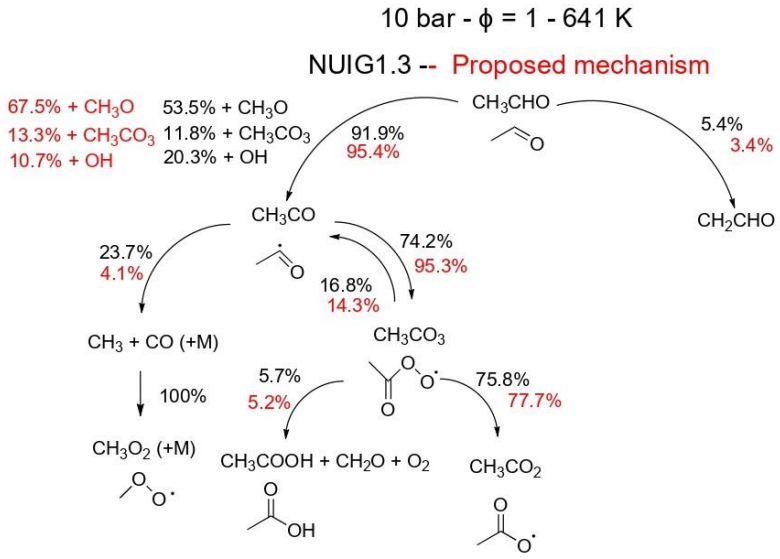

Scheme 4. ROP analysis under Pc=10 bar, ϕ=1.0 and Tc=641 K, when the 10% of the fuel had been consumed. In black are represented the production ratios of the base model and in red those for the proposed model in this study.

6.2 Validation against RCM IDTs

After modifying the NUIG1.3 model, we tested the performance of the updated model against the measured data in this work and IDT measurements from Tao et al. [12]. Figure 10 shows simulations performed with the original NUIG1.3 model, the modified mechanism, and IDT measurements obtained in this work in the RCM. The graph compares the predicted and measured IDT under two conditions: Pc=20 bar, ϕ=1, and Pc=20 bar, ϕ=1.5. Figure 11 shows FS simulations and corresponding experimental measurements for the same conditions as in Figure 4. Finally, Figures 12 and 13 show IDT and FS results, respectively, for experiments conducted at 10 bar and ϕ=1.

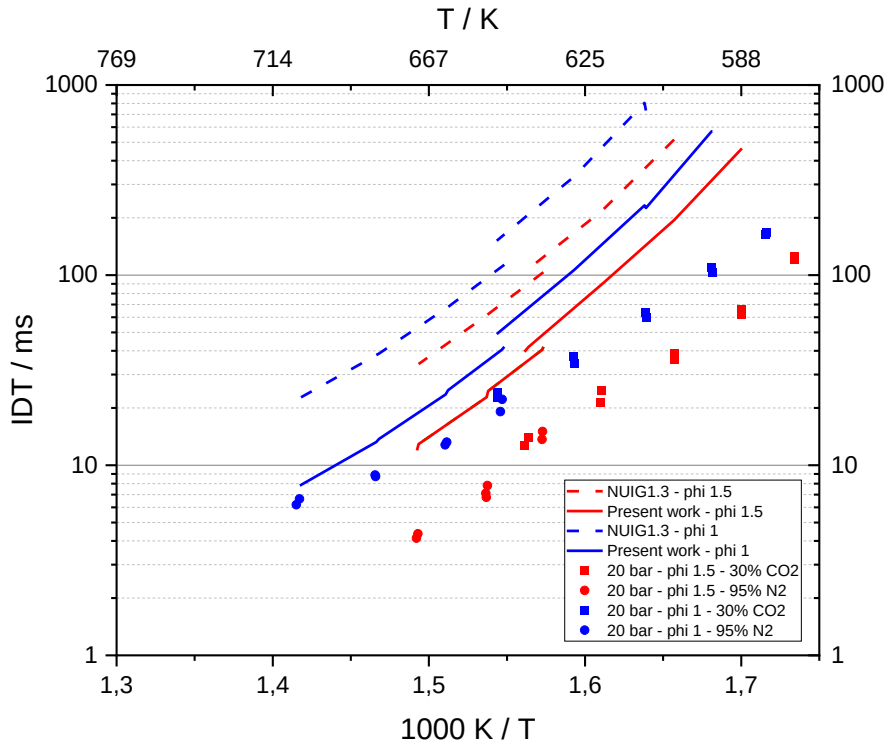

Figure 10. Ignition delay time predicted by NUIG1.3 (dashed line) and the present work (solid line), at two conditions: Pc=20 bar, ϕ=1 and Pc=20 bar, ϕ=1.5. Experiments are represented by points.

At the conditions shown in Figure 10, original IDT predictions were about five times longer than the experimental values. However, after applying the modifications listed in Table 3, the accuracy of the predictions improved significantly. For the mixture with ϕ=1 and C3 as bath gas composition, the predictions were reasonably close, although still slightly slower than the experimental results. In the case of experiments with C4 as bath gas composition, the modifications succeeded in shortening the IDTs, but the improvement was less effective compared to C3 composition.

For the mixture with ϕ=1.5, we were able to reduce the discrepancy between predictions and experimental results by almost half, although the predictions were still significantly off. The trend observed was similar to that for the ϕ=1 mixture, but in this case the mid-low temperature range showed worse accuracy. The low temperature range remained the most challenging in terms of accurately matching the experimental data. Overall, despite the improvements, the predictions at lower temperatures remain further away from the experimental values.

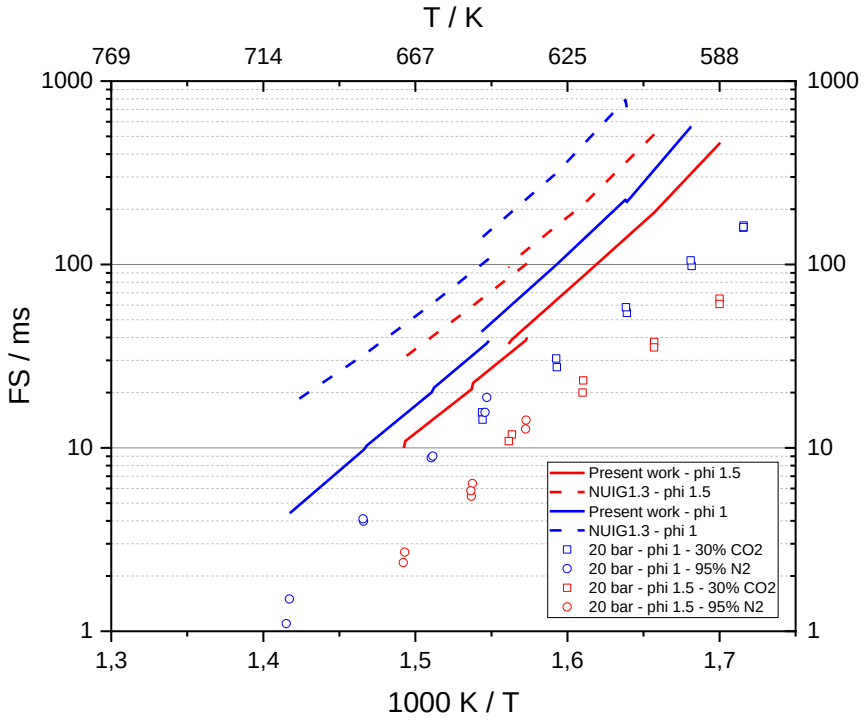

Figure 11. The first stage predicted by NUIG1.3 (dashed line) and the present work (solid line) at two conditions: Pc=20 bar, ϕ=1 and Pc=20 bar, ϕ=1.5. Experimental first stages are represented by points.

The performance of the updated model in predicting the onset of the first stage ignition was also evaluated. As shown in Figure 11, the improvements were slightly more pronounced in the ϕ = 1 condition compared to the ϕ = 1.5 condition, similar to the trends observed in the IDT predictions (see Figure 10). However, in both conditions, the predictions still did not closely match the experimental results, suggesting that further adjustments may be necessary to accurately capture the behavior under these conditions.

In Figure 12, the IDT is analyzed under different conditions: Pc = 10 bar and ϕ = 1. At this pressure and equivalence ratio, the behavior of the model proposed in this work is also tested in the high temperature range. Between 700 and 800 K, the modified model predictions show increased reactivity compared to the experiments, resulting in faster IDTs than expected. However, for temperature below 700 K, the model provides more accurate results, with IDTs slightly longer than the experimental values. It is important to note that the proposed model predicts ignitions at lower temperatures compared to the original model, which is in better agreement with the experimental data. In the high temperature range, despite the adjustments made (as shown in Table 3), the modifications did not significantly affect the behavior of the original NUIG1.3 mechanism. This is because the reactions selected for modification were deliberately chosen for their low sensitivity at higher temperatures, ensuring minimal impact in this temperature regime.

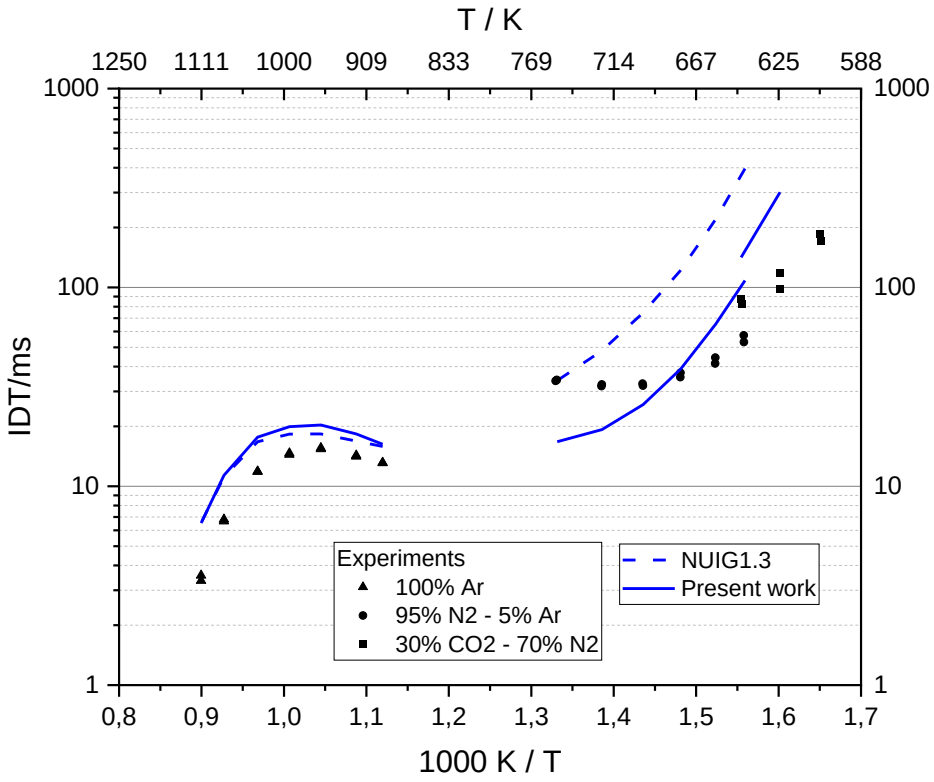

Figure 12. Ignition delay times predicted by NUIG1.3 (dashed line) and the present work (solid line) at Pc=10 bar and ϕ=1. Experimental IDTs are represented by points.

Our model also evaluated its performance for FS under the conditions of 10 bar and ϕ = 1, with the results shown in Figure 13. Under these conditions, FS shows the most significant improvement compared to the other parameters. In section 3 of this study, we discussed the behavior of the available mechanisms against the measured data, and for FS, no major differences were observed between the mechanisms, all showing inaccurate predictions. However, after implementing the modifications in our work, a substantial improvement in FS predictions is evident, reducing the discrepancy from about an order of magnitude slower to values much closer to the experimental results. In addition, the model can predict the FS over a wider temperature range. The improved performance of the model under these conditions was expected, as the adjustments to the kinetic model were primarily based on analysis specific to this temperature and pressure range.

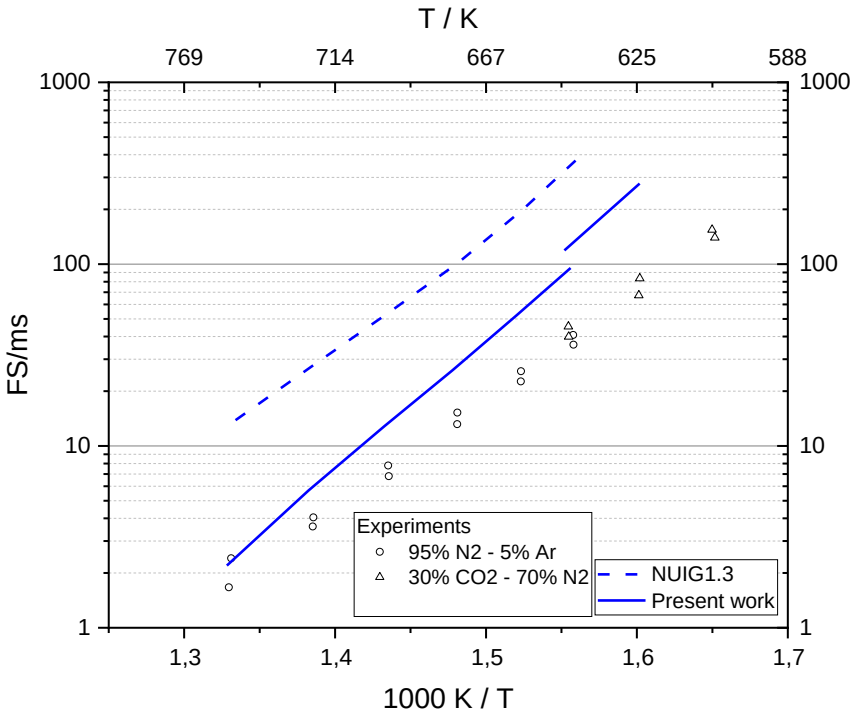

Figure 13. First stages predicted by NUIG1.3 (dashed line) and the present work (solid line) at Pc=10 bar and ϕ=1. Experimental IDTs are represented by points.

Finally, Tao et al. [12] performed IDT measurements 10 bar, ϕ=1, dilution ratio of 13 in the NTC range (830-1100 K) without significant heat release prior to the end of compression, a condition that could not be achieved in our machine, as discussed in section 2. This discrepancy is likely due to the fact that Tao's RCM is able to compress the gas mixture 40% faster than our facility, allowing the chemical reactions to occur predominantly after the end of compression. To evaluate the performance of the modified model in this region, IDT simulations were conducted using the volume profiles provided in [12].

Figure 14 shows the predicted IDT using our model and the original mechanism compared to the IDT data measured by Tao [12]. As shown in Figure 14, both mechanisms exhibit similar behavior in the NTC region. The effects of the applied modifications become noticeable at temperatures below 800 K, which is in line with expectations, since the proposed modifications were designed to improve the model performance in the low temperature range. This behavior suggests that the reaction rates considered become less sensitive in the intermediate temperature regime.

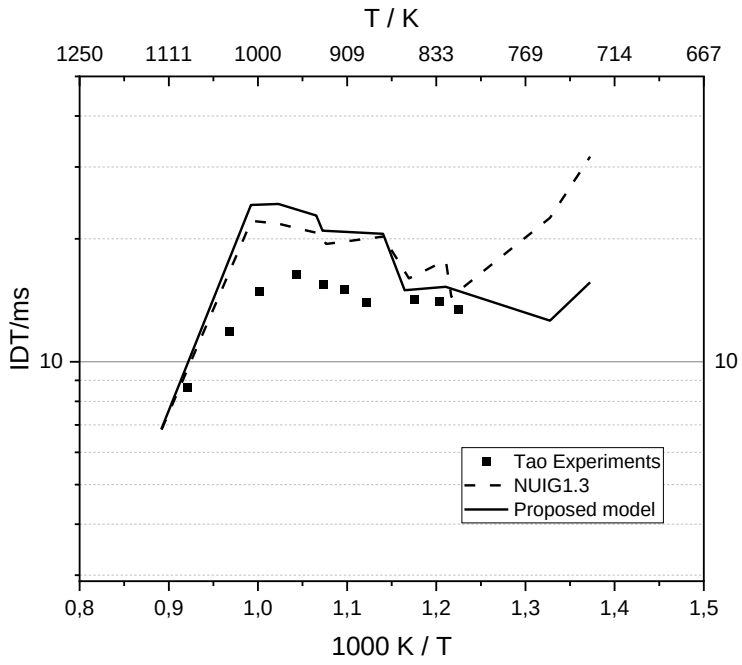

Figure 14. Simulation of Tao experiments with NUIG1.3 model and proposed model.

6.3 Validation against JSR data

IDT data serve as macroscopic validation targets, providing critical insight into the auto-ignition behavior of the species under study. For comprehensive validation of kinetic models, the concentration profiles of intermediate species are essential, providing a more intrinsic assessment of the oxidation chemistry at play. The JSR, an ideal continuous stirred tank reactor, is well suited for this purpose. It is particularly effective for studying the low temperature oxidation chemistry of hydrocarbons and oxygenated fuels. These studies involve monitoring the conversion rates of the reactants and the mole fractions of the reaction products as a function of various parameters, including reaction temperature, residence time, pressure and composition of the inlet gas mixture.

In this study, we evaluate the performance of our kinetic model in comparison to the base mechanism using JSR species concentration measurements from Tao et al. [15] for acetaldehyde lean mixtures (equivalence ratio, ϕ = 0.5; argon dilution ratio of 85%). Experimental conditions range from 528 K to 946 K, with a constant pressure of 700 Torr and a fixed residence time of approximately 3 s.

Figure 15 shows the molar fractions of selected species as a function of temperature. The species included in the graph were chosen because they are the most abundant intermediates formed during the oxidation of acetaldehyde. These intermediates play a critical role in the overall reaction mechanism and provide important insights into the oxidation process. The graphs include the experimental data represented as dots; the

predictions of the NUIG1.3 mechanism, represented as a dashed line; and the results of the model proposed in this study, represented as a solid line.

The first graph shows species with similar concentrations. For argon, there is no noticeable difference between the mechanisms, and both fit the experimental data well. For O_2, the proposed model improves on the base model up to about 900 K. Beyond this temperature, however, neither mechanism accurately predicts the molar fraction, and both underestimate the actual O_2 present. For CO, the predictions are accurate in the low temperature region. However, between 600 K and 700 K, the models predict less CO production than is observed experimentally. Overall, for this species, there is no significant difference between the proposed model and the NUIG1.3 base model.

For H_2O, a slight improvement is observed with the proposed model compared to the base model. However, the predictions do not follow accurately the trend observed in the experiments: up to about 680 K the H_2O production is underestimated, while beyond 680 K the model starts to overestimate the H_2O production. This suggests that while there is some improvement in predicting the overall trend, further refinement may be needed to accurately capture H_2O behavior across the temperature range.

Methane production in the modified model shows no significant difference from the base model, indicating that this aspect of the mechanism remains unchanged. However, for CH_3O_2H there is a slight improvement in the prediction at lower temperatures. Despite this improvement, the model still fails to capture the peak concentration observed in the experimental data at 600 K, suggesting that further modifications may be required.

The CH_3OH plot shows a significant improvement in the low temperature range, as the modified model corrects the underestimation of methanol production seen in the base model. However, despite this improvement at lower temperatures, the performance of the model declines beyond 600 K, consistently overestimating methanol production at higher temperatures. The maximum molar fraction predicted by the modified model is about twice the value observed in the experimental measurements. In this case, the base model shows a much better fit to the experimental data than the modified model.

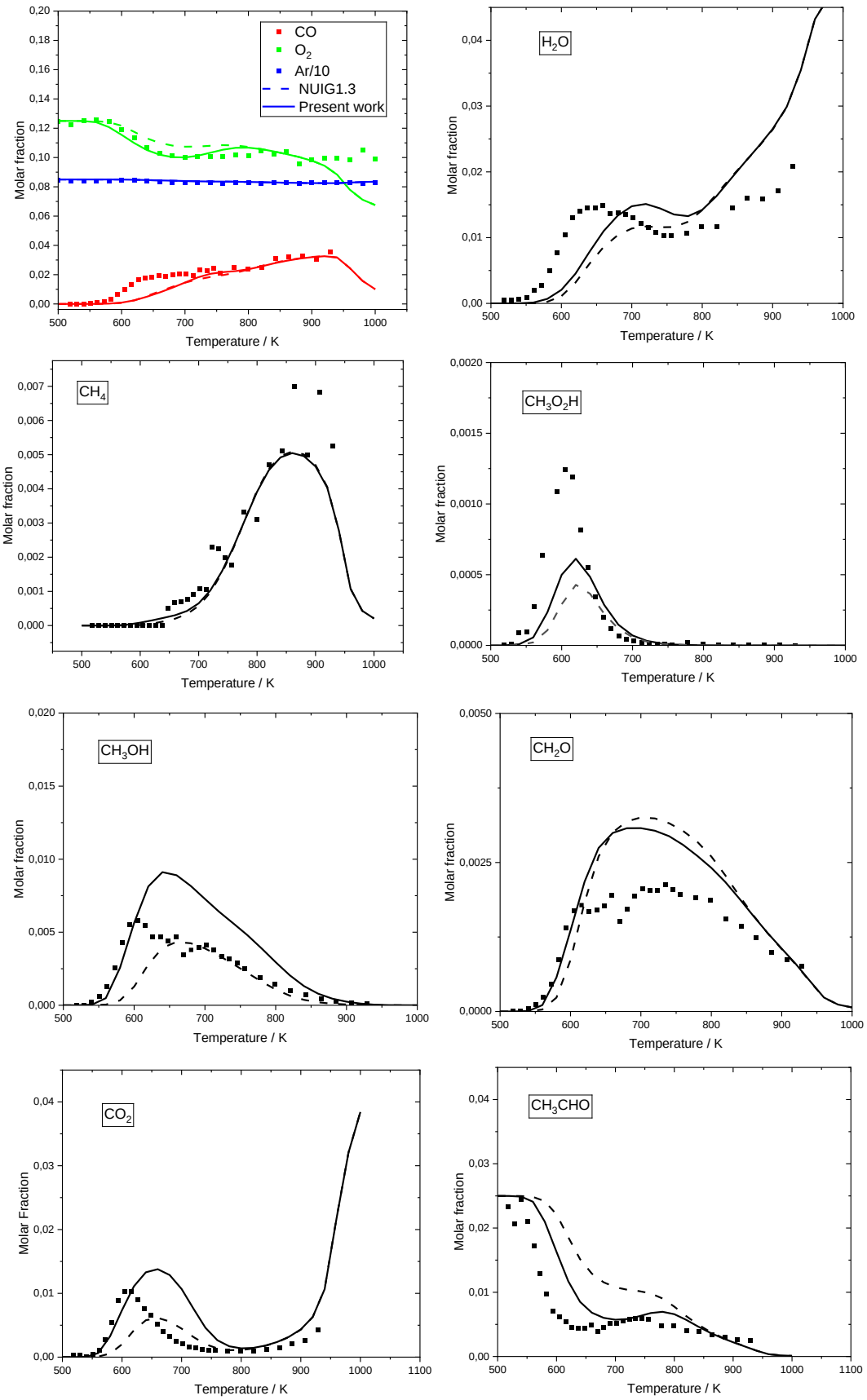

Figure 15. JSR species measurement at ϕ=0.5, Ar dilution ratio of 85%, P=700Torr. Solid line represents present work, dashed line represents NUIG1.3 model and the points represent the experimental results.

For CH_2O. a slight improvement in prediction is observed, which is sufficient to accurately describe its behavior in the low temperature range. Beyond 600 K, the experimental measurements show little variation in the CH_2O concentration, while both the base and modified models significantly overpredict the molar fraction over the entire temperature range.

A similar trend is observed for CO_2. Up to 600 K, the modified model provides a more accurate prediction of CO_2 production. However, between 600 K and 800 K there is a significant overestimation of the CO_2 concentration compared to both the experimental data and the base model. Beyond 800 K, both models behave similarly and agree with the experimental measurements, showing comparable CO_2 concentrations.

The last plot shows the molar fraction of acetaldehyde. The modified model provides a consistently better prediction over the entire temperature range, especially in the low temperature range where it closely follows the experimental data. Beyond 800 K, the consumption predicted by the modified model and the original model are quite similar and in agreement with the experimental data.

In conclusion, the proposed model provides more accurate predictions in the low temperature range, and for most of the species analyzed, the modified model outperforms the base model, providing better agreement with experimental data. However, in the higher temperature range (750 to 900 K), the model tends to overestimate the production of certain species compared to experimental observations. Future investigations will require IDT data in this temperature range at different pressures and equivalence ratios to fully understand acetaldehyde oxidation chemistry in the NTC regime. Nevertheless, this analysis represents a significant improvement in the low temperature oxidation chemistry of acetaldehyde and provides first-ever validation targets in the RCM under these conditions.

7 Conclusion

In this study, IDT experiments for acetaldehyde mixtures were performed using a RCM under three conditions: Pc=10 bar and ϕ=1.0, Pc=20 bar and ϕ=1.0 and Pc=20 bar and ϕ=1.5. These measurements were used to evaluate kinetic models available in the literature, showing that only the model proposed by Tao and NUIGMech mechanisms performed reasonably well at high temperatures. At lower temperatures, however, all evaluated models significantly underpredicted the reactivity of acetaldehyde compared to the experimental data. Overall, NUIG1.3 was identified as the most accurate. Using the experimental data and the NUIG1.3 mechanism, the influence of pressure and equivalence ratio was analyzed. As predicted by the theory, both the simulations and the experimental results indicated that increasing pressure and fuel concentrations shortened the IDT. ROP analyses were performed, showing that in the low temperature range, the most significant reaction pathway for acetaldehyde involves HAA at the alpha position, followed by addition to O_2. As the temperature increases, HAA reactions at the beta position and decomposition reactions play a more important role. Sensitivity analysis allowed identifying the most sensitive reactions influencing the IDT and FS at measured conditions, concluding that at 10 bar, in the low range of temperature, the most sensitive reaction with a positive sensitivity coefficient was the radical decomposition of CH_3CO into CH_3 and CO, meanwhile the most sensitive with a negative coefficient was the addition to O_2 of CH_3CO. In the high temperature range the most sensitive reactions found with the highest positive and negative sensitivity coefficient were the radical decomposition of CH_2CHO into CH_3 and CO and the HAA at alpha position of acetaldehyde in combination with HO_2, respectively. No meaningful differences between different Pc and equivalence ratio were appreciated in the sensitivity analysis. Based on these results, preliminary modifications were made to the NUIG1.3 model to improve its predictions in the low temperature range. These modifications focused primarily on CH_3CO chemistry and alpha-position HHA reactions. The adjustments were aimed at increasing the importance of the CH_3CO addition to O_2 in the reaction mechanism, with the goal of increasing the overall reactivity at these conditions. The model predictions were in better agreement to the measured data using the modified model compared to the original mechanism. However, the discrepancies between model predictions and experimental data remain significant for most of the low-temperature conditions. The model consistently underestimated reactivity in this regime, indicating a need for further investigation at low temperatures. Simulations of Tao's IDT experiments showed that the modifications had no significant effect on the NTC regime. Both the base and modified mechanisms predicted slightly longer IDTs compared to the experimental data. In LT JSR evaluations using Tao's data, the modified model showed improved performance relative to the base model, but deficiencies remained in the mid-temperature range. While an improvement was observed at low temperatures above 600 K, the model overpredicted several key species involved in acetaldehyde oxidation. In conclusion, this study provides valuable IDT data for acetaldehyde under previously unexplored conditions, highlighting the limitations of existing kinetic models. Further research is required to improve our

understanding of the chemistry of acetaldehyde oxidation, particularly in the low to moderate temperature range.

Declaration of Generative AI and AI-assisted technologies in the writing process

During the preparation of this work I used DeepL Write in order to improve readability and language. After using this tool, I reviewed and edited the content as needed and take full responsibility for the content of the publication.

References

[1] Dubie, R. (2019). Paris Agreement (United Nations Framework Convention on Climate Change). In *Geography Today: An Encyclopedia of Concepts, Issues, and Technology* (pp. 326–327). Bloomsbury Publishing Plc.

[2] Seitz, H. K., & Stickel, F. (2010, June). Acetaldehyde as an underestimated risk factor for cancer development: Role of genetics in ethanol metabolism. *Genes and Nutrition*. https://doi.org/10.1007/s12263-009-0154-1

[3] Skinner, G. B., & Ruehrwein, R. A. (1959). Shock tube studies on the pyrolysis and oxidation of methane. *Journal of Physical Chemistry*, *63*(10), 1736–1742. https://doi.org/10.1021/j150580a040

[4] Dagaut, P., Reuillon, M., Voisin, D., Cathonnet, M., Mcguinness, M., & Simmie, J. M. (1995). Acetaldehyde Oxidation in a JSR and Ignition in Shock Waves: Experimental and Comprehensive Kinetic Modeling. *Combustion Science and Technology*, *107*(4–6), 301–316. https://doi.org/10.1080/00102209508907809

[5] Yasunaga, K., Kubo, S., Hoshlkawa, H., Kamesawa, T., & Hidaka, Y. (2008). Shock-tube and modeling study of acetaldehyde pyrolysis and oxidation. *International Journal of Chemical Kinetics*, *40*(2), 73–102. https://doi.org/10.1002/kin.20294

[6] Mével, R., Chatelain, K., Blanquart, G., & Shepherd, J. E. (2018). An updated reaction model for the high-temperature pyrolysis and oxidation of acetaldehyde. *Fuel*, *217*, 226–239. https://doi.org/10.1016/j.fuel.2017.12.060

[7] Hidaka, Y., Kubo, S., Hoshikawa, T., & Wakamatsu, H. (2005). Shock-tube study of acetaldehyde pyrolysis.

[8] Bentz, T., Striebel, F., & Olzmann, M. (2008). Shock-tube study of the thermal decomposition of CH3CHO and CH3CHO + H reaction. *Journal of Physical Chemistry A*, *112*(27), 6120–6124. https://doi.org/10.1021/jp802030z

[9] Won, S.J., Ryu, J.C., Bae, J.H., Kim, Y.D., & Gang, J. (2000). Shock-Tube Study of the Oxidation of Acetaldehyde at High Temperature. *Bulletin of The Korean Chemical Society, 21*, 487-492.

[10] Shrestha, K. P., Giri, B. R., Adil, M., Seidel, L., Zeuch, T., Farooq, A., & Mauss, F. (2021). Detailed Chemical Kinetic Study of Acetaldehyde Oxidation and Its Interaction

with NOx. *Energy and Fuels*, *35*(18), 14963–14983. https://doi.org/10.1021/acs.energyfuels.1c01948

[11] Griffiths, J. F. and Hasko, S. (1984). Two-stage ignitions during rapid compression: spontaneous combustion in lean fuel-air mixtures. Proceedings of the Royal Society of London. A. Mathematical and Physical Sciences, 393(1805), 371-395. https://doi.org/10.1098/rspa.1984.0063

[12] Tao, T., Kang, S., Sun, W., Wang, J., Liao, H., Moshammer, K., … Yang, B. (2018). A further experimental and modeling study of acetaldehyde combustion kinetics. *Combustion and Flame*, *196*, 337–350. https://doi.org/10.1016/j.combustflame.2018.06.007

[13] Nourani Najafi, S. B., Gersen, S., Hashemi, H., Glarborg, P., Mokhov, A. V., & Levinsky, H. B. (2024). Autoignition enhancement of methane by admixture of low fraction of acetaldehyde: simulations and RCM experiments in stoichiometric and rich mixtures. *International Journal of Chemical Kinetics*, *56*(9), 534-548. https://doi.org/10.1002/kin.21727

[14] Zhang, X., Ye, L., Li, Y., Zhang, Y., Cao, C., Yang, J., … Qi, F. (2018). Acetaldehyde oxidation at low and intermediate temperatures: An experimental and kinetic modeling investigation. *Combustion and Flame*, *191*, 431–441. https://doi.org/10.1016/j.combustflame.2018.01.027

[15] Tao, T., Sun, W., Hansen, N., Jasper, A. W., Moshammer, K., Chen, B., … Yang, B. (2018). Exploring the negative temperature coefficient behavior of acetaldehyde based on detailed intermediate measurements in a jet-stirred reactor. *Combustion and Flame*, *192*, 120–129. https://doi.org/10.1016/j.combustflame.2018.01.048

[16] Hashemi, H., Christensen, J. M., Marshall, P., & Glarborg, P. (2021). Acetaldehyde oxidation at elevated pressure. *Proceedings of the Combustion Institute*, *38*(1), 269–278. https://doi.org/10.1016/j.proci.2020.06.311

[17] *Internal Combustion Engines Improving Performance, Fuel Economy and Emissions*. (2020). *Internal Combustion Engines Improving Performance, Fuel Economy and Emissions*. MDPI. https://doi.org/10.3390/books978-3-03936-169-4

[18] Leplat, N., & Vandooren, J. (2010). Experimental Investigation and Numerical Simulation of the Structure of CH3CHO/O2/Ar Flames at Different Equivalence Ratios. *Combustion Science and Technology, 182*, 436 - 448.

[19] Marinov, N. M. (1999). A Detailed Chemical Kinetic Model for High Temperature Ethanol Oxidation. *International Journal of Chemical Kinetics*, *31*(2–3), 183–220. https://doi.org/10.1002/(sici)1097-4601(1999)31:3<183::aid-kin3>3.0.co;2-x

[20] Christensen, M., Abebe, M. T., Nilsson, E. J. K., & Konnov, A. A. (2015). Kinetics of premixed acetaldehyde + air flames. *Proceedings of the Combustion Institute*, *35*(1), 499–506. https://doi.org/10.1016/j.proci.2014.06.136

[21] Tao, T., Sun, W., Yang, B., Hansen, N., Moshammer, K., & Law, C. K. (2017). Investigation of the chemical structures of laminar premixed flames fueled by acetaldehyde. *Proceedings of the Combustion Institute*, *36*(1), 1287–1294. https://doi.org/10.1016/j.proci.2016.05.030

[22] Lee, C., Vranckx, S., Heufer, K. A., Khomik, S. V., Uygun, Y., Olivier, H., & Fernandes, R. X. (2012). On the chemical kinetics of ethanol oxidation: Shock tube, rapid compression machine and detailed modeling study. *Zeitschrift Fur Physikalische Chemie*, *226*(1), 1–27. https://doi.org/10.1524/zpch.2012.0185

[23] Junji Furukawa, Takeo Saegusa, Hiroyasu Fujii, Polymerization of Acetaldehyde, Bulletin of The Japan Petroleum Institute, 1961, Volume 3, Pages 33-38, Released on J-STAGE December 26, 2008, Print ISSN 0582-4656, https://doi.org/10.1627/jpi1959.3.33, https://www.jstage.jst.go.jp/article/jpi1959/3/0/3_0_33/_article/-char/en

[24] Ramalingam, A., Zhang, K., Dhongde, A., Virnich, L., Sankhla, H., Curran, H., & Heufer, A. (2017). An RCM experimental and modeling study on CH4 and CH4/C2H6 oxidation at pressures up to 160 bar. *Fuel*, *206*, 325–333. https://doi.org/10.1016/j.fuel.2017.06.005

[25] Goodwin, D.G., Moffat, H., & Speth, R.L. (2016). Cantera: An Object-oriented Software Toolkit for Chemical Kinetics, Thermodynamics, and Transport Processes. Version 2.2.1.

[26] Pan, J., Wei, H., Shu, G., Chen, Z., & Zhao, P. (2016). The role of low temperature chemistry in combustion mode development under elevated pressures. *Combustion and Flame*, *174*, 179–193. https://doi.org/10.1016/j.combustflame.2016.09.012

[27] Wu, Y., Panigrahy, S., Sahu, A. B., Bariki, C., Beeckmann, J., Liang, J., … Curran, H. J. (2021). Understanding the antagonistic effect of methanol as a component in surrogate fuel models: A case study of methanol/n-heptane mixtures. *Combustion and Flame*, *226*, 229–242. https://doi.org/10.1016/j.combustflame.2020.12.006

[28] Ramalingam, A., Panigrahy, S., Fenard, Y., Curran, H., & Heufer, K. A. (2021). A chemical kinetic perspective on the low-temperature oxidation of propane/propene mixtures through experiments and kinetic analyses. *Combustion and Flame*, *223*, 361–375. https://doi.org/10.1016/j.combustflame.2020.10.020

[29] Baigmohammadi, M., Patel, V., Nagaraja, S., Ramalingam, A., Martinez, S., Panigrahy, S., … Curran, H. J. (2020). Comprehensive Experimental and Simulation Study of the Ignition Delay Time Characteristics of Binary Blended Methane, Ethane, and Ethylene over a Wide Range of Temperature, Pressure, Equivalence Ratio, and Dilution. *Energy and Fuels*, *34*(7), 8808–8823. https://doi.org/10.1021/acs.energyfuels.0c00960

[30] Nagaraja, S. S., Liang, J., Dong, S., Panigrahy, S., Sahu, A., Kukkadapu, G., … Curran, H. J. (2020). A hierarchical single-pulse shock tube pyrolysis study of C2–C6 1-

alkenes. *Combustion and Flame*, *219*, 456–466. https://doi.org/10.1016/j.combustflame.2020.06.021

[31] Lokachari, N., Panigrahy, S., Kukkadapu, G., Kim, G., Vasu, S. S., Pitz, W. J., & Curran, H. J. (2020). The influence of iso-butene kinetics on the reactivity of di-isobutylene and iso-octane. *Combustion and Flame*, *222*, 186–195. https://doi.org/10.1016/j.combustflame.2020.08.007

[32] Panigrahy, S., Liang, J., Nagaraja, S. S., Zuo, Z., Kim, G., Dong, S., … Curran, H. J. (2021). A comprehensive experimental and improved kinetic modeling study on the pyrolysis and oxidation of propyne. *Proceedings of the Combustion Institute*, *38*(1), 479–488. https://doi.org/10.1016/j.proci.2020.06.320

[33] A. Abd El-Sabor Mohamed, S. Panigrahy, A.B. Sahu, G. Bourque, H.J. Curran, An experimental and modeling study of the auto-ignition of natural gas blends containing C1-C7 n-alkanes, Proceedings of the Combustion Institute 38 (2021) accepted.

[34] Nagaraja, S. S., Power, J., Kukkadapu, G., Dong, S., Wagnon, S. W., Pitz, W. J., & Curran, H. J. (2021). A single pulse shock tube study of pentene isomer pyrolysis. *Proceedings of the Combustion Institute*, *38*(1), 881–889. https://doi.org/10.1016/j.proci.2020.06.069

[35] Dong, S., Zhang, K., Senecal, P. K., Kukkadapu, G., Wagnon, S. W., Barrett, S., … Curran, H. J. (2021). A comparative reactivity study of 1-alkene fuels from ethylene to 1-heptene. *Proceedings of the Combustion Institute*, *38*(1), 611–619. https://doi.org/10.1016/j.proci.2020.07.053

[36] Dong, S., Zhang, K., Ninnemann, E. M., Najjar, A., Kukkadapu, G., Baker, J., … Curran, H. J. (2021). A comprehensive experimental and kinetic modeling study of 1- and 2-pentene. *Combustion and Flame*, *223*, 166–180. https://doi.org/10.1016/j.combustflame.2020.09.012

[37] Nagaraja, S. S., Kukkadapu, G., Panigrahy, S., Liang, J., Lu, H., Pitz, W. J., & Curran, H. J. (2020). A pyrolysis study of allylic hydrocarbon fuels. *International Journal of Chemical Kinetics*, *52*(12), 964–978. https://doi.org/10.1002/kin.21414

[38] El-Sabor Mohamed, A. A., Sahu, A. B., Panigrahy, S., Baigmohammadi, M., Bourque, G., & Curran, H. (2022). The effect of the addition of nitrogen oxides on the oxidation of propane: An experimental and modeling study. *Combustion and Flame*, *245*. https://doi.org/10.1016/j.combustflame.2022.112306

[39] Panigrahy, S., Mohamed, A. A. E. S., Wang, P., Bourque, G., & Curran, H. J. (2023). When hydrogen is slower than methane to ignite. *Proceedings of the Combustion Institute*, *39*(1), 253–263. https://doi.org/10.1016/j.proci.2022.08.025

[40] Lu, H., Dong, S., Liu, F., Nagaraja, S. S., Lindblade, N., Turner, M. A., … Curran, H. J. (2023). A wide-range experimental and kinetic modeling study of the pyrolysis and

oxidation of 1-butyne. *Proceedings of the Combustion Institute*, *39*(1), 355–364. https://doi.org/10.1016/j.proci.2022.09.044

[41] Lu, H., Liu, F., Nagaraja, S. S., Dong, S., Turner, M. A., Mathieu, O., … Curran, H. J. (2023). A wide-range experimental and kinetic modeling study of the pyrolysis and oxidation of 2-butyne. *Proceedings of the Combustion Institute*, *39*(1), 157–167. https://doi.org/10.1016/j.proci.2022.07.147

[42] Dong, S., Wang, B., Jiang, Z., Cheng, X., Liu, B., Wang, H., … Curran, H. (2023). On the low-temperature chemistry of 1,3-butadiene. *Proceedings of the Combustion Institute*, *39*(1), 365–373. https://doi.org/10.1016/j.proci.2022.09.046

[43] Mittal, G., & Sung, C. J. (2006). Aerodynamics inside a rapid compression machine. *Combustion and Flame*, *145*(1–2), 160–180. https://doi.org/10.1016/j.combustflame.2005.10.019

[44] Li, Y., Zhou, C. W., Somers, K. P., Zhang, K., & Curran, H. J. (2017). The oxidation of 2-butene: A high pressure ignition delay, kinetic modeling study and reactivity comparison with isobutene and 1-butene. *Proceedings of the Combustion Institute*, *36*(1), 403–411. https://doi.org/10.1016/j.proci.2016.05.052

[45] Gururajan, V., & Egolfopoulos, F. N. (2019). Direct sensitivity analysis for ignition delay times. *Combustion and Flame*, *209*, 478–480. https://doi.org/10.1016/j.combustflame.2019.08.007

[46] Warnatz, J. (2000). Hydrocarbon oxidation high-temperature chemistry. In *Pure and Applied Chemistry* (Vol. 72, pp. 2101–2110). Walter de Gruyter GmbH. https://doi.org/10.1351/pac200072112101